NASA CR-176,788

aer

Final Report
Contract No. NASW-4062

An Investigation of the Energy Balance of Solar Active Regions Using the ACRIM Irradiance Data

ATMOSPHERIC AND ENVIRONMENTAL RESEARCH, INC.
CAMBRIDGE, MASSACHUSETTS

P127fr

Final Report
Contract No. NASW-4062

An Investigation of the Energy Balance of Solar Active Regions Using the ACRIM Irradiance Data

Larry D. Petro
Atmospheric and Environmental Research, Inc.
840 Memorial Drive
Cambridge, MA 02139

Prepared for:

National Aeronautics and Space Administration
Solar Maximum Mission Guest Investigator Program

TABLE OF CONTENTS

		Page
1.	INTRODUCTION	1
2.	WORK COMPLETED DURING THE CONTRACT PERIOD	1
	2.1 Influence of Faculae on Solar Irradiance	1
	2.2 Model of the Influence of Sunspots on Solar Irradiance	2
	2.3 Observations of the Influence of Sunspots on Solar Irradiance	3
	2.4 Observations of Large-Scale Heat-Flow Inhomogeneities	4

APPENDICES (Papers submitted for publication)

A. "A Photometric Search for Giant Solar Convection Cells," W.-H. Chiang, L. D. Petro, and P. V. Foukal.

B. "The Influence of Faculae on Total Solar Irradiance and Luminosity," P. Foukal and J. Lean

C. "Physical Interpretation of Variations in Total Solar Irradiance," P. Foukal

1. INTRODUCTION

This report fulfills the required submission of a final report under NASA contract NASW-4062, "An Investigation of the Energy Balance of Solar Active Regions Using the ACRIM Irradiance Data." During the contract period Dr. Larry Petro replaced Dr. Peter Foukal as principal investigator as a result of Dr. Foukal's leaving his position at AER, Inc. As approved in a letter from the Contracting Officer on Sept. 4, 1985, a portion of the work to be carried out under NASW-4062 was subcontracted to Cambridge Research and Instrumentation, Inc., which is Dr. Foukal's present place of employment. The work performed under the contract resulted in the submission of three papers for publication in scientific journals. These papers are attached in an appendix to the final report and the results obtained are summarized in the appropriate following sections. All work described in this report was carried out in consultation with Dr. Foukal.

2. WORK COMPLETED DURING THE CONTRACT PERIOD

2.1 Influence of Faculae on Solar Irradiance

A paper entitled "The Influence of Faculae on Total Solar Irradiance and Luminosity" was completed by Dr. Foukal and collaborator Dr. Judith Lean and will be published in the March 15, 1986, issue of the Astrophysical Journal. The paper presents the detection of a significant correlation between the solar irradiance, corrected for the flux deficit due to sunspots, and both the 205-nm flux and a photometric facular index. This suggests that faculae contribute significantly to the total solar flux. However, errors in the sunspot correction could contribute to the correlation, since most of the variance of the uncorrected signal is due to sunspots. A detailed analysis presented in the paper supports facular emission as the more likely source of correlation with the corrected radiances, rather than error in the sunspot correction. Further measurements demonstrate that faculae and sunspots make approximately equal, but opposite sense, contributions to the total irradiance on an active region time scale during the spot-maximum year, 1980. However, arguments are presented that these two contributions are independent, and therefore facular emission is not simply reradiated sunspot-blocked flux.

A paper, based upon an invited review talk at the San Francisco meeting of the American Geophysical Union, has been submitted by Dr. Foukal to the

Journal of Geophysical Research (Atmospheres). This paper, entitled "Physical Interpretation of Variations in Total Solar Irradiance," will appear in a proposed Special Collection on Solar Variability. This review concludes that more precise observations of the total solar irradiance and radius over long time scales are required to test models that would enable interpretation and prediction of small perturbances of S caused by perturbations of the solar convection zone.

2.2 Model of the Influence of Sunspots on Solar Irradiance

A consultant under the contract, Dr. Eric Graham, provided a computer program which simulates two-dimensional convection in a compressible, statified medium. This program was successfully run at AER by Dr. Wei-Hwan Chiang on a Cromemco CS-1, MC68000-based, microcomputer. A velocity field previously calculated by Dr. Graham with an earlier version of the code (J. Fluid Mech., 70, 1975, 689) was reproduced on the microcomputer in a verification run which required 15 CPU-hours and employed a 9 cell by 16 cell grid for the finite difference scheme. This run attained a convective steady state as demonstrated in Figure 1 by the evolution of the Nusselt number. The final state consisted of two counter-rotating convection cells as shown in Figure 2.

Dr. Graham also completed subroutines to calculate ionization and other thermodynamic variables. These subroutines and the two-dimensional compressible convection code are now operating on an IBM-PC. Dr. Graham has undertaken to place the thermodynamic subroutines into operation with the convection program, to include a radiative photospheric boundary, and to include sunspot body forces. The original plan of work proposed these tasks to be accomplished at AER, but the complexity of the required program modifications and the level of effort required to complete the work described in Section 2.4 led to the agreement by Dr. Graham to undertake this extra work at no extra cost. At this writing, the tasks are not completed but are expected to be so by mid-March, 1986.

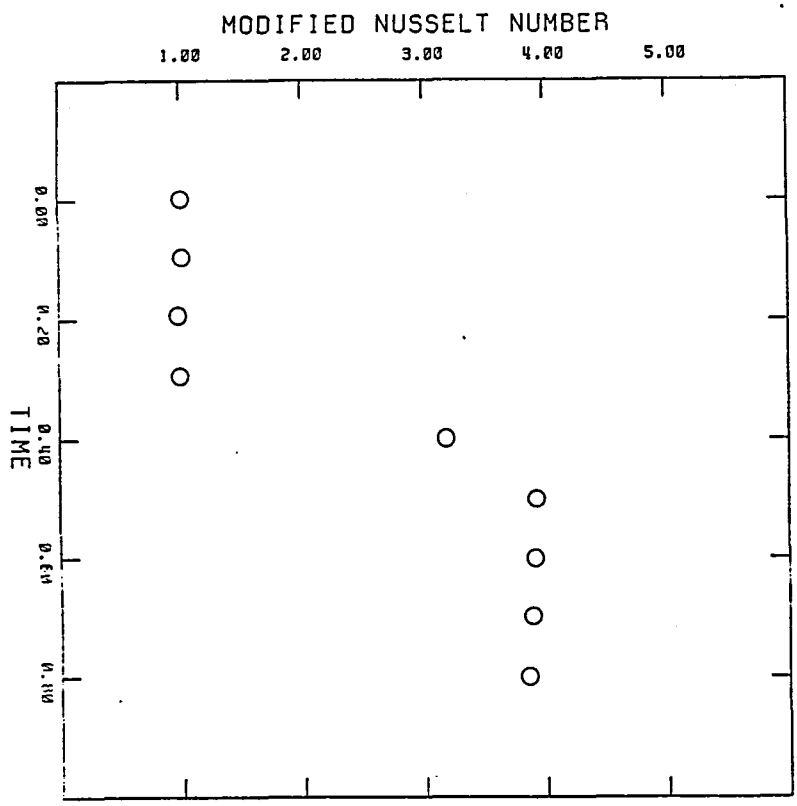

Fig. 1. Evolution of the Nusselt Number during a numerical simulation, using a microcomputer, of two-dimensional convection in a compressible, stratified medium. The computer code was provided by Dr. E. Graham.

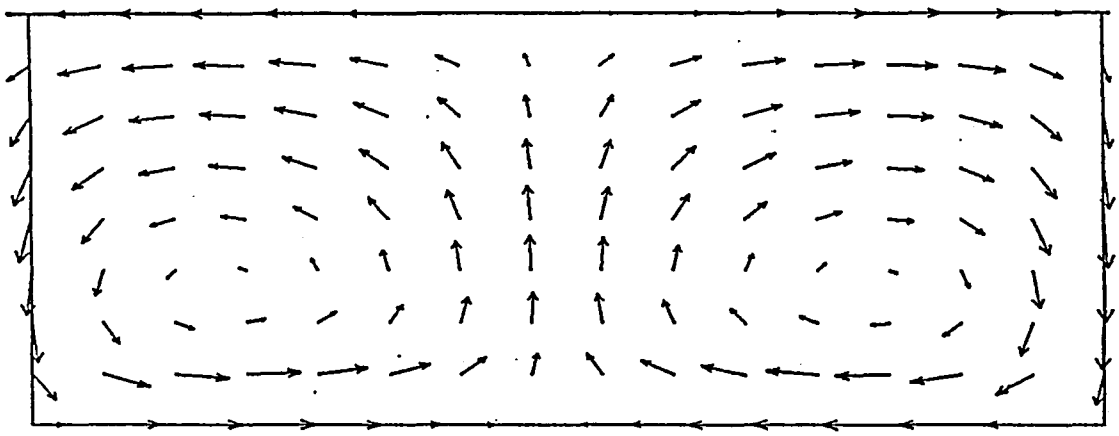

Fig. 2. Velocity field of the steady-state convection for the case illustrated in Figure 2. The grid is 9 cells by 16 cells.

2.3 Observations of the Influence of Sunspots on Solar Irradiance

Equipment to perform high-precision, white-light observations of sunspot areas was acquired by Dr. Foukal and procedures were tested, but as yet no measurements have been obtained. These observations were seriously impeded by the lack of large sunspots during this time of solar-cycle minimum and by poor weather.

Tests were carried out with a five-inch aperture Carroll spar borrowed from Williams College (with the assistance of Dr. J. Pasachoff) and was housed in a shed on a Northeastern University site in Nahant, Massachusetts. This arrangement proved cumbersome. Careful comparison of a 3.5-inch aperture Questar reflector and 4.0-inch aperture Unitron refractor was undertaken. This demonstrated that the Unitron telescope scatters less light (a desirable feature for accurate sunspot area measurements), and it was therefore purchased. A 35-mm camera and an evaporated-chromium neutral-density filter were also obtained, the latter allowing the full-aperture resolution (1.2 arcseconds) to be utilized while readily achieving proper exposure.

Good-quality photoheliograms in white light have been obtained with the Unitron refractor which are suitable for area and coordinate measurements of accuracy comparable to similar data obtained with full-disk patrols at SPO, BBSO, and elsewhere. An attempt to extract sunspot areas from measurements of film negatives with a computerized P.D.S. microdensitometer at American Science and Engineering was deemed unsuccessful due to the large amount of computer post-processing required. Therefore, it was decided to employ a simple measurement procedure using calibrated enlargements of the original photographic negatives: first the spots are located with respect to a heliographic grid and then their area is graphically measured. The project will be continued using sunspot areas reported by NOAA. The observing program will be continued during this year with the present equipment.

An observing run was carried out at Sacramento Peak Observatory by Dr. Petro, and, in collaboration with L. Gilliam of SPO, procedures and computer programs were developed to obtain sunspot bright ring photometry. Analysis of this data at SPO by Dr. Petro identified deficiencies in the flat-field procedure, which is necessary for high precision surface photometry. Improved CCD observations of sunspot bright rings were obtained in a cooperative arrangement with the National Solar Observatory at Sacramento Peak. These new obser-

vations should include better flat field scenes. However, analysis of these new data was not carried out in order that the work described in Section 2.4 could be completed.

2.4 Observations of Large-Scale Heat-Flow Inhomogeneities

A paper entitled "A Photometric Search for Solar Giant Convection Cells" has been prepared by Drs. Petro, Chiang, and Foukal and submitted to Solar Physics. The paper presents the analysis of observations which were obtained in May 1985 at the Vacuum Telescope of the National Solar Observatory on Kitt Peak, Arizona. A detailed statistical analysis of the combined data from 15 days of observation limits the r.m.s. of the hypothesized giant cell pattern to be less than 0.23 K. This limit is ten times more restrictive than the similarly-derived limit of 3 K found earlier (Foukal and Fowler, 1984, Ap. J., 281, 442), and is comparable to estimates based upon recent nonlinear numerical convection models by Glatzmaier (private communication). The implication of this work for ACRIM measurements is that the contribution of giant cells to the r.m.s. of the solar irradiance is less than three parts in 10^6 on one-month time scales.

APPENDIX A

A Photometric Search for Solar Giant Convection Cells

W.-H. Chiang and L. D. Petro
Atmospheric and Environmental Research, Inc., 840 Memorial Drive,
Cambridge, Massachusetts 02139

P. V. Foukal
Cambridge Research and Instrumentation, Inc., 20 Erie Street,
Cambridge, Massachusetts 02139

Submitted to Solar Physics
26 February 1986

Abstract

We limit the photometric contrast of solar giant convection cells using λ525.6 nm continuum images obtained on 15 days in May 1985. The r.m.s. of the giant cell intensity pattern must be less than or equal to the observed r.m.s. on spatial scales 80 Mm to 240 Mm which is 0.023 percent or, equivalently, 0.33 K. However, the spatial scale and exposure dependence of the variance demonstrate that giant cells are not the source of the observed variance. Consequently, a tighter constraint on the r.m.s. of the giant cell pattern may be placed, namely 0.016 percent or 0.23 K. This limit is consistent with temperature perturbations estimated from recent non-linear simulations of global-scale solar convection. We use this limit on the r.m.s. of the giant cell pattern to estimate that the contribution of giant cells to the fluctuation of the solar irradiance on a one-month time scale is less than 3×10^{-5} S.

1. Introduction

The solar convective modes that transport heat and angular momentum most efficiently have proven difficult to identify directly from observations of the photospheric velocity field, although their scales and geometry are critical in understanding the dynamics of the Sun's luminosity variation and its magnetic cycle. In the absence of clear observational results, theoretical efforts have been directed toward studies of solar convection dynamics based on plausible assumptions for the values of effective viscosity and thermal conductivity (see reviews by Gilman, 1986; Durney, 1976).

Results from such calculations have been applied to understanding mechanisms responsible for photospheric differential rotation (e.g., Gilman, 1986; Glatzmaier, 1984) and global heat flux variations (Gilman, 1978). More recently, the equations for an MHD dynamo have also been included in the models to simulate the solar cycle behavior of the magnetic field (e.g., Gilman, 1986; Glatzmaier, 1984).

The velocity fields of order 100 m s^{-1} predicted by these models have been compared to photospheric Doppler velocity data over spatial scales comparable to the scale of the most unstable modes. The predicted velocities are an order of magnitude larger than those observed in the most complete analyses (e.g., Snodgrass and Howard, 1984), although a detection at the 25 m s^{-1} level has been claimed (Scherrer et al., 1986). The velocity amplitudes expected at the photosphere are uncertain due to the possibility of strong smoothing of large-scale velocity gradients by smaller convective scales near the top of the convection zone (Stix, 1981; van Ballegooijen, 1985).

Relatively little has been done to test the models through photometric investigation of the expected photospheric temperature perturbations. A direct search on the disk for the temperature perturbations expected at low latitudes should place more restrictive constraints on models of global-scale convection than can be expected from measurements (e.g., Koutchmy et al., 1977; Kuhn et al., 1985) of the pole-equator temperature difference. The relevance of the pole-equator temperature difference to global-scale convection has been discussed by Durney (1976). A previous study (Foukal and Fowler, 1984) of continuum photometric data placed an upper limit of 3 K on temperature perturbations over spatial scales, L, greater than 50 Mm but less than 200 Mm. This limit was much smaller than the 10 K - 100 K suggested by

linearized convection simulations (Glatzmaier and Gilman, 1981). However, recent nonlinear calculations (Glatzmaier, 1984) indicate temperature perturbations smaller than 10 K.

In this paper we compare recent theoretical values (Glatzmaier, 1984) with significantly more sensitive photometric results we obtained and point out some temperature constraints that should be particularly useful for future numerical simulations at lower viscosity.

2. Observational Procedure and Data Reduction

The results presented here are based upon digital images obtained with the National Solar Observatory Vacuum Telescope located on Kitt Peak, Arizona. This telescope illuminates the curved entrance slit of an 11 m focal length Littrow spectrometer with a 33.6 cm image of the Sun. The image is scanned in a direction perpendicular to the projected rotation axis of the Sun. For these observations a 512-diode Reticon (TM) detector in the spectrometer focal plane sampled the λ525.6 nm intensity of the solar surface along a segment which is approximately one-quarter of the solar diameter in length. Scans of 2048 × 512 samples were obtained which covered an area which extended slightly beyond the east and west limbs and from the equator to one-half solar radius either north or south. Four such scans were obtained north of the equator and four south of the equator during a two-hour interval on each of the 15 days of observation between 1 and 28 May 1985. Weather or instrumental malfunction prevented observations from being obtained on the remaining 13 days during this interval. A journal of the times of observation and the central meridian longitudes (L_o) is presented in Table 1.

Table 1

Journal of Observations

U.T. Date (May 1985)	L_o (deg)	U.T. Date (May 1985)	L_o (deg)	U.T. Date (May 1985)	L_o (deg)
1.77	159	12.77	14	21.69	256
2.71	147	13.69	2	24.81	215
6.87	92	18.73	295	25.74	202
10.86	39	19.82	281	26.81	188
11.75	27	20.69	269	28.69	163

The data were corrected at the telescope for dark current and gain and further geometrically and photometrically corrected by us before forming maps in heliographic coordinates of the residual intensity. The mathematical models and procedures employed to accomplish this are described in the following subsections.

2.1 Geometric Rectification

Constants to describe the geometrical distortions of the solar disk image were determined from the observed position of the solar limb, assuming that the true limb is a circle. For computational speed and simplicity we defined the limb as those points whose intensity is 0.2 that of the intensity at the center of the image. A right-hand Cartesian coordinate system was defined in the image plane with x increasing in the scan direction and y in the perpendicular direction. Curvature of the spectrometer entrance slit (β), the position angle of the slit (α), the ratio of measurement scales in the two orthogonal directions (k), and the position of the center of the disk (x_o, y_o) were determined from a least squares fit to the observed limb positions. The square of the measured distance to the limb (r_i) for a raw limb position (x_i', y_i') is, corrected for the above effects,

$$r_i^2 = [kx_i' + \alpha y_i' + \beta(y_i' - 256)^2 - x_o]^2 + [y_i' - y_o]^2.$$

We adjusted the above parameters to minimize $\Sigma\ (R^2 - r_i^2)^2$, where R is the fitted radius of the circle, for approximately 600 positions (x_i', y_i') per scan.

The fitted parameters (k, α, β, x_o, y_o, and R) were used to transform and bin the raw 2048 × 512-pixel images into 256 × 64-pixel images whose row and column indices correspond to a Cartesian coordinate system and for which the radius of the solar disk was 127 pixels. An additional 4 times reduction of the amount of data to be further processed was accomplished by adding the four binned scans of each hemisphere on each day. The subsequent photometric correction of the images was greatly facilitated by the 128 times reduction of the amount of data and by the geometric standardization. The granulation noise also was reduced by binning and adding the scans.

2.2 Photometric Correction

Photometric corrections were applied to account for small variations of the diode gains and offsets, for atmospheric transmission variation, and for telescope vignetting. The method of correction required an estimate of the true intensity at each point of observation. This was approximated by the tabular limb-darkening function which consisted of the observed intensity binned in 128 equal increments of $\mu = \cos\theta$ (θ = heliocentric angle of a point of observation). For the detection of giant cells this was a very good estimate since the giant cell pattern does not share the spatial scale or symmetry of the assumed limb-darkening or photometric-correction functions.

The photometric model of the observed intensity at pixel (i,j) in terms of the response of the diodes and of the atmospheric transparency was:

$$I_{obs} = I_{true}\ (a + b\ i + c\ j)\ \gamma_j + i_{o,j},$$

where the transparency variation was modeled by a linear spatial function (a + b i + c j) and each diode was modeled by an independent gain (γ_j) and offset ($i_{o,j}$). With I_{true} given by the empirical limb-darkening function, this model was fitted by the method of least squares to determine the parameters of the model. The diode gains and offsets required corrections of order one percent and the transparency required corrections of order a few tenths of a percent.

A vignetting function was determined separately for each hemisphere by adding the fifteen northern and the fifteen southern scans. This provided a good estimate of the vignetting function since this process reduced (due to solar rotation) the amplitude of any random solar pattern with feature size smaller than ~ 150 Mm by $(15)^{-1/2}$, whereas a stable telescope vignetting function did not so suffer. The magnitude of the vignetting correction was typically of order 0.1 percent. Therefore, the transmission on day k, V_k, was represented by:

$$V_k(i,j) = 1 + \varepsilon_k \, v(i,j).$$

This form assumed that the shape of the vignetting error, v(i,j), did not change from day to day, but that the amplitude ε could have. The observed dispersion of ε was ± 17 percent.

The limb-darkening and correction functions were determined iteratively, which was a rapidly convergent process since the corrections were small and essentially decoupled. Pixels within a projected distance of 0.75 solar radius of the center of the disk (i.e., $\mu > 0.66$) were employed to determine the free parameters of the photometric model for each image. The images of magnetic regions identified from limb-darkening residual images and the daily NSO and Mt. Wilson magnetograms (Solar-Geophysical Data, 1985) were excluded from the photometric modeling.

2.3 Heliographic Maps

Maps in heliographic coordinates were prepared from the residuals from the empirical limb-darkening function for the 30 photometrically corrected scans. Those portions of the disk images greater than a projected distance of 0.75 solar radii from the center of the disk were excluded from the map, but not the previously noted magnetic regions. The maps comprised 256 × 64 cells and covered a range of 360° in longitude and ± 35° in latitude about the equator. The projected dimensions (at the solar equator) of a map cell (longitude × latitude) were 1.41° × 1.09° or 17.2 Mm × 13.4 Mm. A typical map cell contained information from approximately 4,700 of the raw-image pixels. The equations of transformation from disk position to heliographic coordinates and the daily solar aspect were taken from The Astronomical Almanac (1985).

To further reduce the noise in the residual map, the data were smoothed with a 5 × 5 running-mean filter, which provided an effective spatial resolution of 86 Mm × 67 Mm. The smoothed map is shown in the upper portion of Figure 1. The map-cell exposure (defined as the number of bins from the 256 × 64 disk images) is mapped in the upper portion of Figure 2.

The local standard deviation was calculated to provide a statistical assessment of the features visible in the smoothed map. To do so, a moving window larger than or comparable to the size of hypothesized giant cells was used, namely 15 cells × 15 cells (258 Mm × 200 Mm). A contour plot of the calculated local standard deviation is shown in the lower portion of Figure 2.

3. Analysis of the Maps

To ascertain whether the photometric effects of giant cells are present in our observations, we examined the smoothed (5 × 5) residual intensity mapped in Figure 1 and analyzed the local standard deviation mapped in Figure 2. We felt this approach was more appropriate than a study of the map power spectrum since extensive areas were contaminated by active regions. Indeed, the most prominent features of the residual map were active regions, which are identified by the NOAA/USAF number of the associated sunspot group (Solar-Geophysical Data, 1985) in the lower portion of Figure 1. Outside the active regions, a low amplitude, noise-like pattern is visible in Figure 1. This pattern could be the result of small-scale noise processes, such as granulation or the network, or could be the sought for giant cell pattern.

The most promising region of the map for the recognition of giant cells was between 120° and 220° longitude since this region contained relatively little magnetic flux, as shown in NSO maps of magnetic flux during Carrington Rotations 1761 and 1762 (J. Harvey, private communication), and was of high exposure (Figure 2) in our residual intensity map. However, no features are present which resemble the anticipated giant cells. The r.m.s. of the intensity residuals in this region and other high-exposure, low-flux regions was less than or equal to 0.023 percent. Since these regions comprised a large portion of the map, we adopted this value as an upper limit on the r.m.s. of the giant cell intensity pattern. The corresponding upper limit on temperature variations at the surface of the Sun was 0.33 K since the ATLAS6 model

(R. Kurucz, private communication) indicates $\Delta I/I \cong 4\ \Delta T_{eff}/T_{eff}$ at λ 525.6 nm.

The rough correspondance between high exposure and low variance noted above suggested that a tighter limit could be placed on the amplitude of a possible giant cell pattern by considering the temporal and spatial properties of the variance. The relationship between local variance and exposure is shown in Figure 3 for the variance of the 5 × 5 smoothed map and the local exposure. The observed relationship was well represented by $\sigma^2 = \sigma_0^2 + \sigma_1^2/E$, where E is the exposure of the unsmoothed map cells. The form of the variance-exposure relationship suggests that two types of features contributed to the variance in the map. The first was independent of exposure (σ_0^2) and must have a lifetime greater than approximately four days. The second (σ_1^2/E) depended upon the inverse of the exposure and was effectively a white noise source, i.e., a source whose coherence time is less than the interval of time between samples, namely one day. The lifetime of the exposure-dependent source of variance did not match the properties of the giant cells and was presumably solar granulation.

The linear relationship between variance and inverse exposure was obeyed by the unsmoothed map as well as maps smoothed by 3 × 3 and 5 × 5 running-mean filters. The values of the fitted parameters σ_0^2 and σ_1^2 for these maps are presented in Table 2.

Table 2

Components of the Map Variance

Smoothing size	σ_0^2 (× 10^{-8})	σ_1^2 (× 10^{-6})
1 × 1	18.5 ± 3.3	11.50 ± 0.53
3 × 3	5.0 ± 1.0	1.81 ± 0.16
5 × 5	2.0 ± 0.4	0.95 ± 0.06

The exposure-independent source of variance was examined, since it could be due to giant cells. Information on the spatial scale of this source was obtained from the dependence of σ_0^2 on the smoothing size. If the scale of

the source of variance were comparable to or greater than the variance window (15 cells × 15 cells or 258 Mm × 200 Mm), then the intrinsic variance would be independent of smoothing scale. This case corresponds to giant cells. However, at the opposite limit, if the scale of the source of the intrinsic variance were equal to or less than the cell size, then the observed variance would vary as N^{-1}, where N = number of cells in the smoothing filter. The first possibility (giant cells) was ruled out by the strong dependence of intrinsic variance on smoothing filter size demonstrated by the data in column 2 of Table 2. The limit of vanishing feature size was not obeyed either, but if the dimensions of the source of variance were 1.6 times the cell size, or a characteristic size of 24 Mm, then the observed dpeendence of σ_o^2 upon smoothing filter size would be reproduced. We did not establish a solar feature which has a lifetime longer than one solar rotation and a size scale of 24 Mm, but in any case, giant cells are ruled out.

The intrinsic variance of the 5 × 5 smoothed map was used to place a more restrictive upper limit on the r.m.s. of the giant cell pattern. Adopting the 2-σ upper limit on σ_o^2(Table 2) the upper limit on the giant cell r.m.s. is 0.016 percent of the intensity at the center of the disk or 0.23 K.

4. Discussion and Conclusions

The main result of this study is that no photospheric temperature variations greater than 0.23 K r.m.s. (2σ upper limit) were observed which can be ascribed to giant cells. Our operational definition of a giant cell pattern is one whose lifetime is greater than a few days and whose feature scale is in the range 80 Mm to 240 Mm. This temperature limit is a factor of 10 more restrictive than that of a previous study (Foukal and Fowler, 1984).

Predictions for the size scale of large, low-latitude convective cells are typically in the range 100 Mm to 300 Mm (Gilman, 1986; Glatzmaier, 1984; van Ballegooijen, 1985). Plots of the entropy variance versus longitudinal wave number for a representative model (Glatzmaier, 1984) predict ΔT to peak for cells of size 300 Mm. Giant cells characteristically take the form of rolls extending to at least ± 35° in latitude. Our observations would have had little difficulty in spatially resolving such cells.

The lifetime of giant cells is predicted to be one to two solar rotations; hence, they should be stationary over the 7-day disk-passage interval

which contributed to any given map cell of Figure 1. The coherence time of a convective pattern might be decreased below even this disk-passage time if dispersive effects discussed by Gilman (1984) were to play an important role, but the simulations indicate that such effects should be unimportant at the low latitudes we observed.

The amplitude of temperature variation predicted by numerical convection models has received less attention than has the velocity field. The only estimates available are based on recent nonlinear simulations of compressible convection in a spherical shell (Glatzmaier, 1984). This simulation predicted variations in the superadiabatic gradient of about 10^{-5} between individual cells at the top of a convective layer which has a constant heat flux upper boundary (Glatzmaier, private communication). Taking these entropy variations as proportional to fractional temperature perturbations, we found $\Delta T \sim 1$ K at the depth of roughly 50 Mm where the model's upper boundary lies. This is a factor 10 to 100 smaller than previous estimates based on linearized calculations (Glatzmaier and Gilman, 1981), but it is comparable to the observational limit (r.m.s. $\lesssim 0.23$ K) placed here.

The temperature variation estimates derived from such spherical shell models must, however, be viewed with caution. First, the "impermeable" dynamical upper boundary condition may significantly modify the temperature field. Second and more important is the limitation of such models to relatively high viscosity due to the computational difficulties encountered if more vigorous convective motions are simulated. More vigorous convection at higher Rayleigh numbers is expected to produce larger temperature perturbations. Third, the lower eddy thermal conductivities that would go along with lower eddy viscosity in these models would be less effective in smoothing out the cell-to-cell variations of interest here (Foukal and Fowler, 1984). The photometric limits on ΔT presented here seem to pose direct constraints on such lower-viscosity models, since our ΔT is comparable to the value predicted by the low Rayleigh number simulations carried out so far.

Finally, the observations presented here may be used to estimate a limit on the contribution of giant cells to the fluctuation of the solar irradiance on the time scales of the giant cell lifetime, which is expected to be of order one month. If we assume that the fluctuation in the number of giant cells, N_{cell}, obeys Poisson statistics, then the temporal fluctuation of the

pattern irradiance will be less than $N_{cell}^{-1/2}$ times the pattern r.m.s. The effective number of cells visible on the disk is of order 36, so the contribution of the giant cells to the irradiance fluctuation will be less than (1/6) (1.6×10^{-4}) S = 3×10^{-5} S.

Acknowledgements

We thank T. Duvall and F. Recely for assistance at Kitt Peak during our remote observations and T. Duvall for helpful discussions. This project was supported by SMM Guest Investigator Contract NASW-4062.

Figure Captions

Figure 1, upper: Map of residual intensity from solar limb darkening. The cell size (longitude × latitude) is 1.41° × 1.09° and the map has been smoothed by a 5 × 5 running-mean filter. The pixel aspect ratio is 1.25 : 1, so that the aspect ratio on the page of solar features is 1.03 : 1. The 16-level, negative image grey scale maps -0.05 percent or less into white and +0.05 percent or greater into black.

Figure 1, lower: Identification of active regions visible in upper map. The ID numbers are the NOAA/USAF numbers of the associated sunspot groups.

Figure 2, upper: Exposure within the residual intensity map. Exposure is defined as the number of bins from the 256 × 64 disk-images added in a given, unsmoothed map cell. White represents no exposure and black represents a value of 50 or greater.

Figure 2, lower: Local standard deviation of residual intensity. Contours are labeled in units of 0.023 percent of the intensity of the center of the disk.

Figure 3: Variance of residual intensity in the 5 × 5 smoothed map as a function of exposure, E. The variance is well represented by $\sigma^2 = \sigma_0^2 + \sigma_1^2/E$.

References

The Astronomical Almanac: 1985, U.S.N.O., U.S. Government Printing Office, Washington, DC.

Durney, B.: 1976, in V. Bumba and J. Kleczek (eds.), IAU Symposium 71, Basic Mechanisms of Solar Activity, D. Reidel Publishing Company, Dordrecht, Holland, p. 243.

Foukal, P., and Fowler, L.: 1984, Ap. J., 281, 442.

Gilman, P.: 1978, Geophys. Astrophys. Fluid Dynamics, 8, 93.

Gilman, P.: 1984, in R. K. Ulrich, J. Harvey, E. J. Rhodes, and J. Toomre (eds.), Solar Seismology from Space, JPL Publication 84-84, Pasadena, Calif., p. 41.

Gilman, P.: 1986, in P. Sturrock (ed.), Physics of the Sun, D. Reidel Publishing Company, Dordrecht, Holland, in press.

Glatzmaier, G.: 1984, J. Computational Phys., 55, 461.

Glatzmaier, G., and Gilman, P.: 1981, Ap. J. Supp., 47, 103.

Koutchmy, S., Koutchmy, D., and Kotov, V.: 1977, Astr. Ap., 59, 189.

Kuhn, J., Libbrecht, K., and Dicke, R.: 1985, Ap. J., 290, 758.

Scherrer, P., Bogart, R., Hoeksema, J., and Yoshimura, H.: 1986, preprint (to appear in Proceedings of NATO Workshop on the Seismology of the Sun and Distant Stars).

Snodgrass, H., and Howard, R.: 1984, Ap. J., 284 , 848.

Solar-Geophysical Data: 1985, Nos. 490 and 491, Part I, U.S. Department of Commerce, Boulder, Colo., U.S.A.

Stix, M.: 1981, Astr. Ap., 93, 339.

van Ballegooijen, A.: 1985, Preprint.

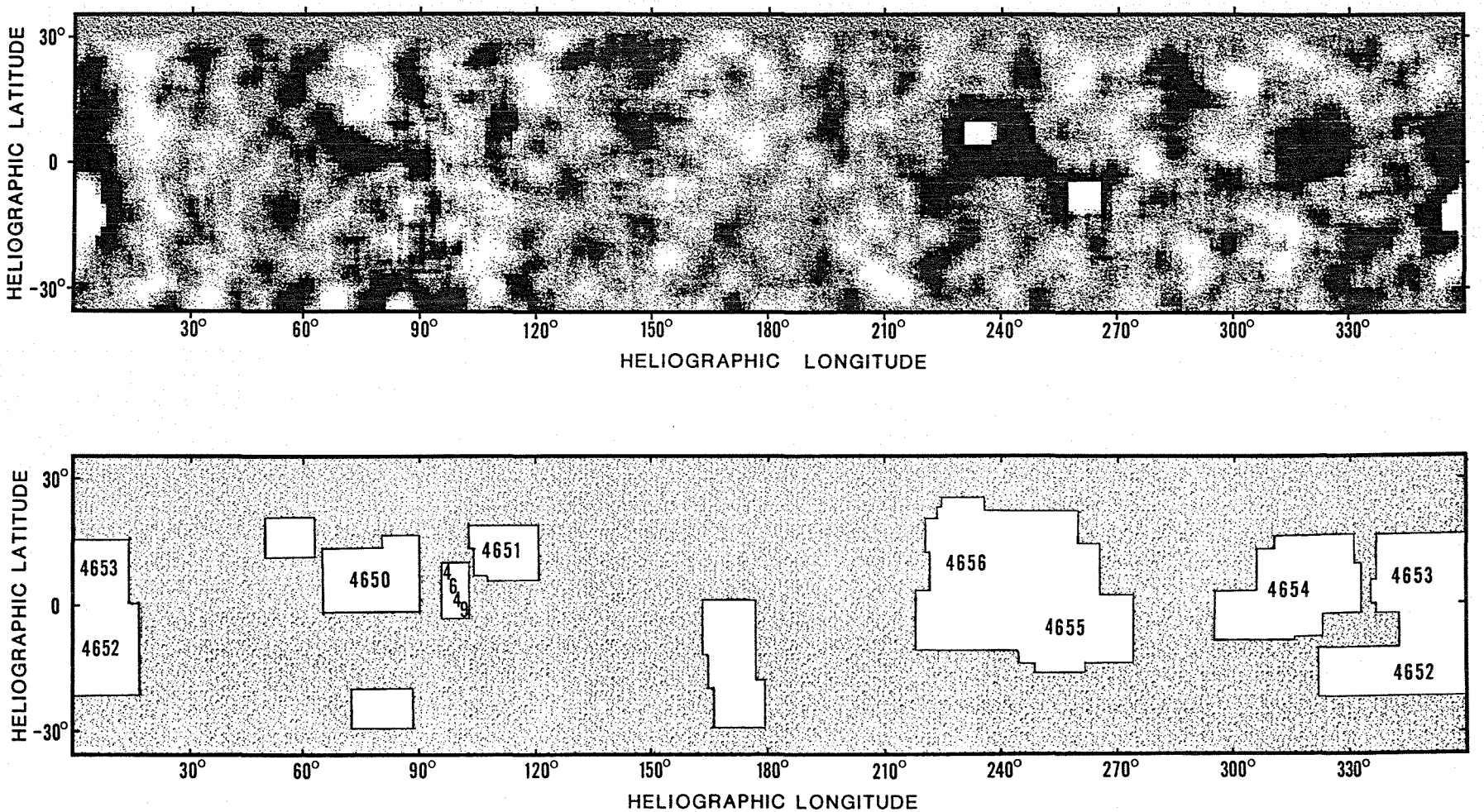
HELIOGRAPHIC LATITUDE
30°
0
-30°
30°
60°
90°
120°
150°
180°
210°
240°
270°
300°
330°
HELIOGRAPHIC LONGITUDE
4653
4652
4650
4651
4656
4655
4654
4653
4652

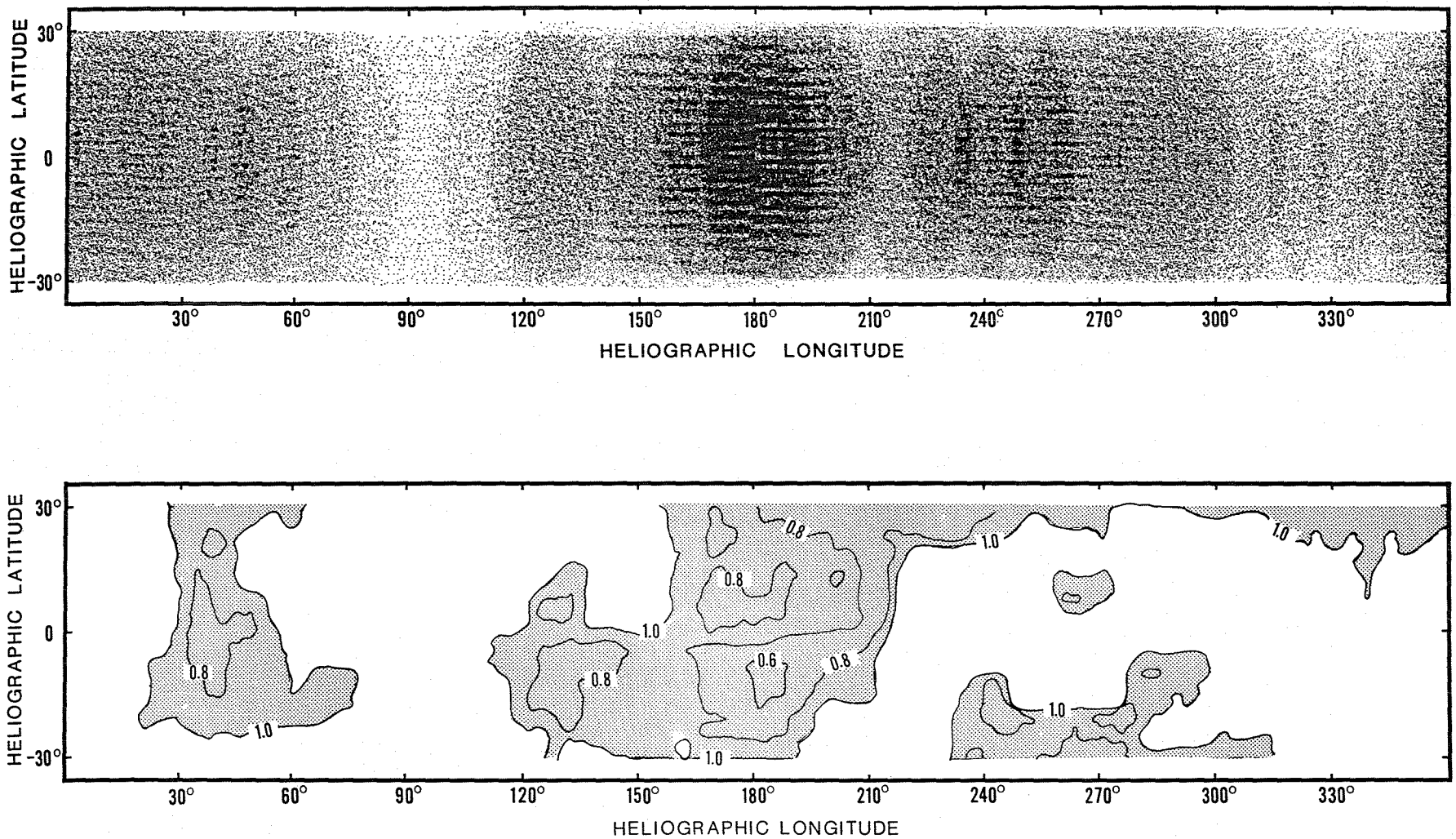
HELIOGRAPHIC LATITUDE
30°
0
-30°
30°
60°
90°
120°
150°
180°
210°
240°
270°
300°
330°
HELIOGRAPHIC LONGITUDE
0.8
1.0
0.6

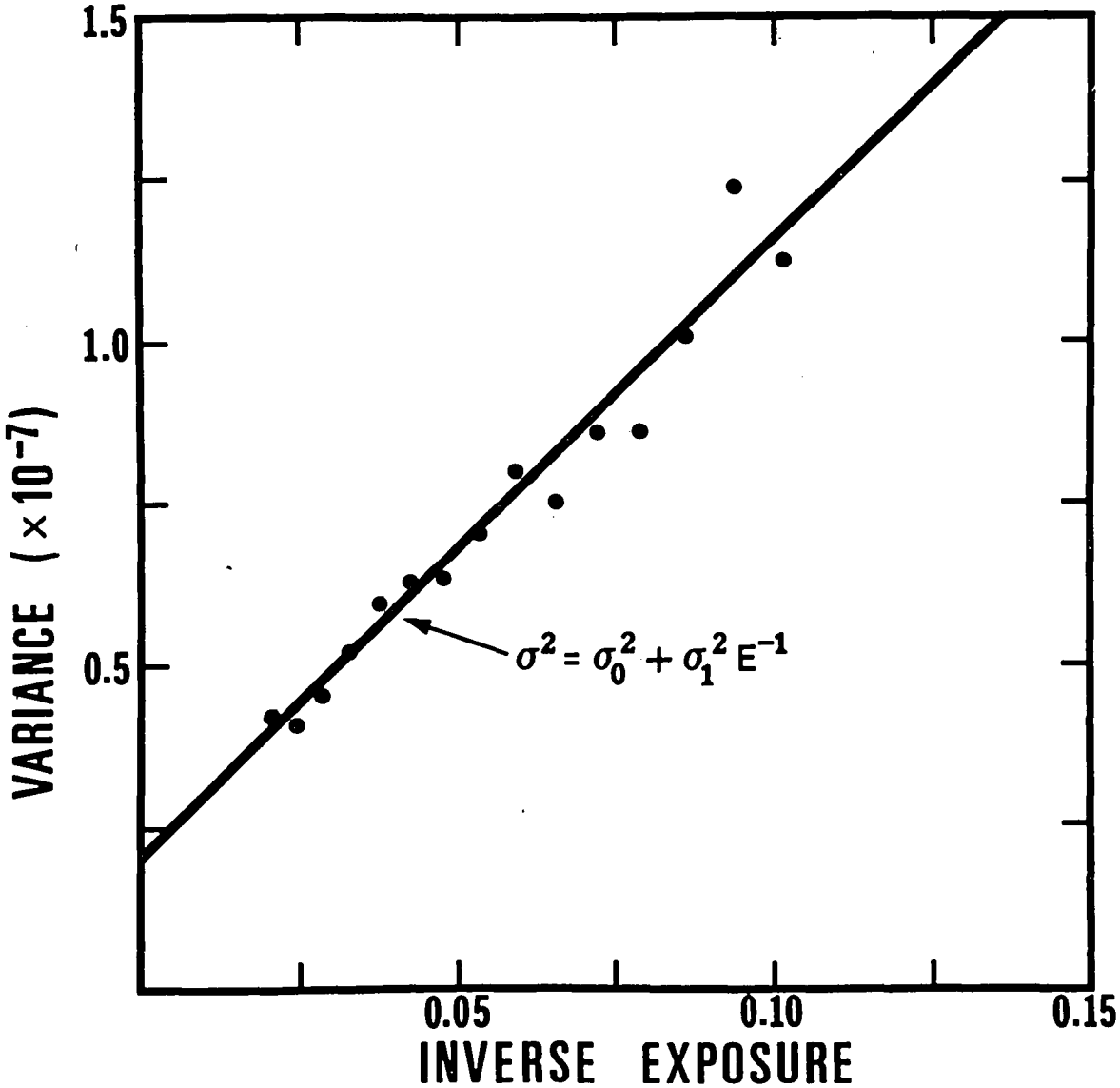
1.5
1.0
0.5
VARIANCE ($\times 10^{-7}$)
$\sigma^2 = \sigma_0^2 + \sigma_1^2 E^{-1}$
0.05
0.10
0.15
INVERSE EXPOSURE

APPENDIX B

The Influence of Faculae on Total Solar Irradiance and Luminosity

P. Foukal

Atmospheric and Environmental Research, Inc.

and

J. Lean

Cooperative Institute for Research in

Environmental Sciences

University of Colorado/NOAA

Submitted to the Astrophysical Journal
July 19, 1985

Abstract

We investigate the facular contribution to the total solar irradiance using the daily ACRIM radiometry for 1980-1982 and the ERB radiometry for 1978-1982. A calculated sunspot blocking function P_s is subtracted from the irradiances, S, and we study the cross-correlation of these residuals $S - P_s$ with the 205 nm ultraviolet flux measured from the Nimbus-7 SBUV experiment, with a white light modulation function P_f calculated from facular areas and contrasts, and with P_s itself. The correlation coefficient at zero lag between the residuals $S-P_s$ and either P_f or the 205 nm flux is about 25% higher than the correlation between $S-P_s$ and P_s. Since the behavior of both P_f and the 205 nm flux are determined by facular rotation and evolution, this suggests that faculae, rather than errors in the P_s function account best for the irradiance residuals. Further evidence for a considerable facular contribution to S is based on the distinct asymmetry of the $S-P_s$ vs 205 nm or P_f cross-correlation functions, on the surprising absence of a 28-day peak in the total irradiance power spectrum, and on analysis of the relative contributions of spot and facular-associated signals to this power spectrum. Time integration of the spot and facular components of irradiance variation indicates that their contributions over time scales of active region evolution were comparable in 1980. We present several arguments based on the thermodynamics of magnetic energy storage, and on the geometry of magnetic connections in active regions and network, which indicate that faculae are not likely to act as conduits for re-radiation of the missing sunspot heat flux. Rather, they seem to represent an independent magnetic perturbation to photospheric heat flow of opposite sign to that of spots, and of comparable magnitude.

I. Introduction

Radiometry from the Solar Maximum Mission (Willson et al. 1981) and Nimbus-7 (Hickey et al. 1980) satellites has shown variations in the total solar irradiance, S, of peak-to-peak amplitude 0.2% over characteristic time scales of roughly 10 days. A substantial fraction of this variance can be explained as the effect of dark sunspots rotating across the photospheric disk (Willson et al. 1981, Foukal 1981, Hoyt and Eddy 1982). The SMM radiometry for 1980 also shows a strong positive correlation with 10.7 cm radio flux, after a calculated variation due to changing projected areas of spots is removed from the total irradiance signal (Hudson and Willson 1981). This correlation led the authors to suggest a facular contribution to the total irradiance variation, although some of the correlation could be caused by error in the calculated sunspot contribution to S, since large faculae are often associated with spot groups. Comparisons of the ACRIM radiometry for 1980 with irradiance variations calculated from intensity maps made in the wings of the FeI λ5250 line, suggest that the facular and spot contributions to S are similar when integrated over time scales of active region evolution (Bruning and Labonte 1983). Evidence presented by Oster et al. (1982) for a strong facular influence on S appears to have been based on a serious overestimate of sunspot areas (Hoyt, Eddy, and Hudson 1983).

It has been known for some time from visible light photometry (e.g., Kiepenheuer 1953; Chapman 1980) that the radiative flux missing in spots can be roughly comparable to the excess flux from faculae in the same active regions. However, this rough agreement has not proven sufficiently compelling to inspire models of spots and faculae as energetically connected phenomena. The ACRIM irradiance record since 1980 and ERB radiometry since 1978 now provide a long, continuous set of irradiance measurements suitable for a more

precise bolometric comparison of spot and facular influences on photospheric heat flow.

The relative facular and spot contributions to S and luminosity, $L_\odot$, also bear directly on studies of possible slow trends in $L_\odot$ over longer time scales of more direct climatological significance. Thus, Fröhlich and Eddy (1984) report evidence for such trends at the level of roughly 0.4% over 11 years. To determine whether such possible trends are likely to involve variations in the output of the quiet sun, it is important to establish whether the component of solar luminosity modulation due to spots and faculae is positively or negatively correlated with the level of solar magnetic activity. This requires that we determine the relative contributions of the spot-associated dips in irradiance and the facula-associated increases in the 11-year signal.

In Section II of this paper we use a one-year subset of the radiometric data to illustrate the basic features of the correlation between short-term variations in total irradiance, ultraviolet flux, and the calculated contributions of spots and faculae. In Section III, we show the full data base used in this study, consisting of radiometric measurements and spot and facular areas from the period 1978-1982, and cross-correlate these data to study the evidence for a facular contribution to S. In Section IV, we present further evidence on the frequency structure and total power of the facular contribution, from power spectrum analysis. In Section V, we compare the magnitude of facular and sunspot contributions to S. In Section VI, we discuss the energy balance of spots and faculae in the broader perspective of other observational and theoretical evidence on their dynamical connection, and we summarize our conclusions in Section VII.

II. Comparison of Variations in Total Irradiance, Ultraviolet Flux, Sunspot Blocking, and White-Light Facular Flux in 1980

Figure 1 shows simultaneous measurements of the total solar irradiance made during 1980 by the ACRIM experiment on the Solar Maximum Mission satellite and the ERB experiment on the Nimbus-7 satellite. Both data sets have been detrended with a 12th order polynomial. Our interest is in the relatively short-term variations of roughly 10-day time scale, whose timing, amplitude, and shape are seen to agree well in the two radiometric records. Since the ACRIM data between February and December 1980 exhibit lower noise, we concentrate in this section on these data.

Figure 2a shows the P_S function that describes the modulation of solar irradiance as calculated from daily projected areas and the estimated photometric contrast of sunspots. The function P_S presented here was calculated by Hoyt (1983, private communication) using procedures and data described by Hoyt and Eddy (1982). Figure 2b shows the 1980 ACRIM radiometry after subtraction of this function P_S. Also plotted in Figure 2 are c) the detrended daily ultraviolet flux F_{uv} measured at 205 nm by the Solar Backscatter Ultraviolet (SBUV) experiment on Nimbus-7 as supplied by D. Heath, and d) a calculated function P_f describing the estimated daily facular contribution to the total irradiance. The function P_f was calculated from daily CaK plage areas provided by the NOAA World Data Center using a limb-brightened bolometric facular contrast (see, e.g., Foukal 1981).

Comparison of the curves 2b and 2c shows close correspondence in the timing of large peaks in the total irradiance residuals and in F_{uv}. Since variations in F_{uv} are known to be caused primarily by the rotation and evolution of faculae (e.g., Heath 1980, Lean et al. 1982), this correlation suggests a facular signal in the total irradiance. The relative amplitude of modulation

seen in F_{uv} is similar to the relative amplitude of peaks and troughs in the total irradiance, which is not surprising since the main contribution to the 205 nm emission is from the same photospheric layers below 400 km above $\tau_{0.5} = 1$ (Vernazza, Avrett, and Loeser 1981), which also determine the facular white light emission. The correspondence in the peak amplitudes shown here is somewhat better than that seen in the comparison of ACRIM radiometry and $F_{10.7}$ presented by Hudson and Willson (1981). This might be expected, since the centimeter wave emission originates at much higher chromospheric and coronal layers.

Comparison of Figures 2a and 2b shows, however, that the time series of (ACRIM-P_S) and P_S are also highly correlated. A substantial contribution to the residuals (ACRIM-P_S) might thus result from errors in P_s, specifically from a systematic underestimate in the spot areas or bolometric contrasts used to calculate P_S. Optimally, to demonstrate a facular signal, we should like to detect a clear increase of S at a time when spot areas were so small that $P_S \sim 0$ (and thus errors in P_S were negligible), while variation in facular area (i.e., in the P_f function plotted in Fig. 2d) was large. The function P_S approaches zero closely in March and August 1980, but the periods of $P_S \sim 0$ are not sufficiently long to separate the facular signal from possible errors in P_S. Examination of the P_S and P_f functions between 1980-82 (when the ACRIM measurements were more noisy) also did not reveal sufficiently extended periods to perform an unambiguous separation.

III. Cross-correlation of the Function S - P_S against -P_s, F_{uv}, and P_f

Since the effect of spots and faculae cannot be directly separated in the data available for this study, we performed a cross-correlation of the residuals against P_S, F_{uv}, and P_f to determine whether faculae or errors in P_S

make the dominant contribution to these residuals. This analysis was carried out using both the three years 1980-1982 of ACRIM data and also for the four years 1978 - 1982 of ERB radiometry. Figure 3 shows the full data base of detrended time series $S - P_S$, P_S, F_{uv}, and P_f used in this cross-correlation study. These cross-correlations, and also the power spectra discussed later, were calculated using statistical routines developed at NOAA by T. Repoff (Heath, Repoff, and Donnelly, 1984).

The cross-correlation functions are shown in Figure 4. The three left panels refer to cross-correlations with $S - P_S$ residuals calculated using ACRIM data for S, the three on the right with $S - P_S$ calculated from ERB data. As expected from the inspection of the 1980 data presented in Section II, $S - P_S$ shows significant positive correlation near zero lag (i.e., correlation coefficient) with each of the three functions $-P_S$, F_{uv}, and P_f. But the correlation at zero lag is noticeably ($\gtrsim$ 25%) higher with either F_{uv} or P_f than with P_S. This higher correlation coefficient supports the qualitative impression obtained from examination of the 1980 data, that the ultraviolet and white-light signatures of faculae reproduce the frequency content and phase of the $S - P_S$ residuals significantly better than would an explanation in terms of errors in P_S.

This explanation of the $S - P_S$ residuals is also supported by the asymmetry of the cross-correlation function of $S - P_S$ against $-P_S$ seen in Fig. 4. The main feature of the asymmetry in panel 4a is the absence (or at least very low amplitude) of even a first cross-correlation peak at positive lag, relative to the amplitude of strong first and second peaks at negative lags. Positive lag is defined to occur when the $S - P_S$ time series leads the second time series. This asymmetry is very noticeable compared to the high degree of symmetry seen in cross-correlation with F_{uv} and P_f. The dashed lines show the

auto-correlation of $S - P_S$ to illustrate the symmetry expected if the two cross-correlated functions were identical.

To interpret this asymmetry, we consider the idealized behavior of the cross-correlation function on various extreme asumptions as to the persistence of the phenomenon that might give rise to the residuals. If $S - P_S$ and S were both generated by a nonrecurring feature, their cross-correlation would exhibit only a central peak. If both were long-lived phenomena recurring at the period P of solar rotation, we would expect a symmetric cross-correlation exhibiting recurrence peaks at both positive and negative lag. This seems to be evident in the cross-correlation of $S - P_S$ against F_{uv} and P_f. If only P_S is caused by a structure that persists for more than one rotation, we find recurrences at positive lag, whereas if only $S - P_S$ is persistent, we find recurrence peaks only at negative lag.

Since the evidence of Fig. 4a seems to be best described by this last situation, we identify the cause of the $S - P_S$ residuals with a solar feature that is much longer-lived than the spots which give rise to P_S variations. The strong peaks at positive lag evident in Fig. 4b and (at least at the first recurrence) in Fig. 4c show that faculae have the required long lifetime. The longer lifetime of faculae compared to spots, by roughly a factor 3, is well known from statistical studies (e.g., Kiepenheuer 1953).

IV. Power Spectrum Analysis

Fig. 5 shows power spectra for four of the five detrended time series plotted in Fig. 3, and also for the detrended ACRIM and ERB radiometry corresponding to the five-year time period 1978-82 of Figure 3. We note first that the total irradiances (Fig. 5a,b) do not exhibit significant power at 28 days, although this period is very prominent in the spectra of the P_S and P_f func-

tion (Fig. 5d,f), in the ultraviolet flux (Fig. 5c) and in the total irradiance after P_S is subtracted (Fig. 5e). A significant peak at 13 days is seen in the ACRIM radiometry, P_S and P_f functions, and most prominently in the F_{uv}. This peak may reflect a tendency for active regions to occupy longitude belts roughly 180° apart, during 1978-1982. Its increased strength in F_{uv} could be due to the limb-brightening of ultraviolet plages, which enhances their visibility roughly ± 6 days of central meridian passage. The four-day peak seen only in the ERB data (Fig. 4b) is a sampling effect caused by the observing schedule of the ERB experiment (C. Fröhlich, private communication).

The absence of a clear 28-day peak in the detrended ACRIM or ERB radiometry may seem surprising in view of the demonstrated modulation of the irradiance by spots whose projected areas (i.e., P_S) show a significant 28-day peak. But it becomes understandable if we remember that the facular and sunspot influences of opposite sign are close to being in phase and so will tend to cancel rather than add in the irradiance time series. Consequently, we expect to find the signal at 28 days to be more closely proportional to the difference in power at 28 days between the P_S and P_f power spectra. The power at 28 days might actually be lower than at adjacent periods where the P_S and P_f power spectra are substantially different. Examination of the ACRIM and ERB power spectra in Fig. 5a,b does indeed show in both cases a definite local minimum in power around 28 days. The amplitude of this relative dip is a rough measure of the difference in contribution by faculae and spots to the total irradiance at 28 days period.

Fig. 6 shows a power spectrum of the $S - P_S$ residuals on an expanded period scale, along with the power in these residuals at each frequency that can be explained by variations in a) $-P_S$ itself, b) F_{uv}, and c) P_f. The results for $S - P_S$ calculated from the ACRIM data are shown in the left panels,

and for the ERB data on the right. These plots show that, at least for the dominant power peak around 28 days, the F_{uv} and P_f variations each can account for roughly 80 percent of the obesrved variance in $S - P_S$ while P_s can account for only about 50 percent. Again, this points to faculae as providing a stronger component of the $S - P_S$ residuals than do errors in P_S. Note that these results are similar for both the ACRIM and ERB residuals.

V. The Relative Magnitude of Time-Integrated Sunspot and Facular Contributions to S

The evidence presented above points to a significant facular influence on the total irradiance. In this section we discuss the magnitude of the time-integrated facular contribution relative to that of spots. We wish to determine whether it is thermodynamically plausible that the heat flux blocked by spots might be balanced over time scales of active region evolution, by excess facular radiation.

To compare these contributions, we divide the total solar irradiance signal S into three components:

$$S = S_o + \Delta S_s + \Delta S_f, \qquad (1)$$

where S_o is the "quiet sun" value of the solar constant in the absence of spots and faculae, and ΔS_s, ΔS_f are respectively the (negative) change in irradiance caused by dark spots and the (positive) change due to faculae. It is convenient to express the measured irradiances as normalized differences from S_{max} the highest solar irradiance signal recorded by the ACRIM in 1980. We then have:

$$S' = \frac{S_{max} - (S_o + \Delta S_s + \Delta S_f)}{S_{max}} \qquad (2)$$

or

$$S' = \left(\frac{S_{max} - S_o}{S_{max}}\right) - \left(\frac{\Delta S_s + \Delta S_f}{S_{max}}\right). \qquad (3)$$

The value of S_{max} is measured from the data before detrending to be 1369.35 watts/m^2 on DOY110 (April 16th). The value of S_o is taken to be 1369.01 watts/m^2, the ACRIM reading on DOY77 (March 17th), when the value of the calculated sunspot blocking P_S was approximately zero (see Fig. 2a) indicating a very low projected area of spots on the disk. The contribution of faculae on that day (estimated by the P_f function) was also relatively low, given the high activity level in 1980 (see Fig. 2d). With these values, we find $(S_{max} - S_o)/S_{max} = 2.5 \times 10^{-4}$. Using this constant difference, the expression (3) can be written as:

$$\frac{\Delta S_s + \Delta S_f}{S_{max}} = 25 \times 10^{-4} - S'. \qquad (4)$$

The time integral of the combined contributions due to spots and faculae is then:

$$\int_{t_1}^{t_2} \left(\frac{\Delta S_s + \Delta S_f}{S_{max}}\right) dt = 2.5 \times 10^{-4} (t_2 - t_1) - \int_{t_1}^{t_2} S' \, dt. \qquad (5)$$

Integration of this expression using ACRIM data (not detrended) yields the values given in Table 1 as a function of t_2 (with t_1 = DOY47). We see from Table 1 that the RHS is always negative as expected if the sunspot blocking exceeds the radiation from faculae. However, the value of S_o adopted here

quite certainly overestimates the true quiet sun irradiance, since considerable facular area was still present on the disk on March 17th. This will cause in turn an underestimate of the first term on the RHS and thus an underestimate of the facular contribution.

The amount of this underestimate can be evaluated using the information contained in the ratio of the P_f functions on DOY110 and DOY77. If we call the "true" quiet sun irradiance S_1, we can write on DOY77:

$$S_o = S_1 + \Delta S'_f \tag{6}$$

since $\Delta S'_s = 0$ on that day. On DOY110 we have:

$$S_{max} = S_1 + \Delta S''_f + \Delta S''_s \ , \tag{7}$$

which yields:

$$\frac{S_{max}-S_1}{S_o-S_1} = \frac{\Delta S''_f + \Delta S''_s}{\Delta S'_f} < \frac{\Delta S''_f}{\Delta S_f} \ , \tag{8}$$

since $\Delta S''_s$ is always negative (and non-zero on DOY110). We can also make the reasonable approximation:

$$\frac{\Delta S''_f}{\Delta S'_f} \simeq \frac{P''_f}{P'_f} \ , \tag{9}$$

since the P_f function should be a good estimate of at least the relative effects of faculae on the total irradiance on the two days. The ratio $P''_f / P'_f \sim 2$ (see Fig. 2d), so, substituting in equations (9) and (8) we have:

$$\frac{S_{max}-S_1}{S_o-S_1} < 2 \ , \qquad (10)$$

and, since:

$$(S_{max}-S_1) = (S_o-S_1) + (S_{max}-S_o) \ , \qquad (11)$$

we find that

$$(S_o-S_1) > (S_{max}-S_o) \ . \qquad (12)$$

It follows that the first term on the RHS of equation (5) is probably at least twice as large as used in Table 1, which is sufficient to approximately balance the facular and spot contributions over the time scales considered here.

VI. Do Faculae Re-radiate the Missing Radiative Flux of Sunspots?

The results obtained above indicate that the sunspot-induced reduction of S is comparable to the excess radiation of faculae over time-scales of active region evolution during 1980. This suggests that energetic balance between spots and faculae is not unreasonable. However, we present in this section several arguments against the view that faculae are conduits for the re-radiation of missing sunspot heat flux, based on considerations that go beyond balance of radiometric contributions to S.

a) Correlation of Spot and Facular Areas

Daily observations of white light faculae and spots over a solar cycle by the Greenwich photoheliograph observers (see the detailed summary of their results given by Kiepenheuer, 1953) show that roughly 10% of all faculae

(by area) are unaccompanied by any discernible spots. This finding comes from the study of large-scale photographic plates on which even small, ephemeral spots were identified. It shows that the spatial correlation of faculae and spots in individual active regions is far from perfect. This can be seen also from the large scatter in a plot of CaK facular areas and white light spot areas on the disc for 1550 days in 1969-1974, based on NOAA-WDC data (Foukal and Vernazza, 1979).

An extreme case of this loose correlation between spot and facular areas on the disc is found in 1913 (J. Eddy, private communication). During that year, which lies at the lowest activity minimum since 1810, the sunspot number was identically zero for three consecutive months in April, May, and June, while facular areas in excess of 250 millionths of the disk area were seen in white light by the Greenwich observers. The white light observations do not reveal faculae inward of $\mu=0.5$, so they underestimate the facular areas that would be measured by CaK observations. Detailed balance of sunspot and facular radiations would then have required storage of sunspot missing flux for three months, before it was re-radiated by faculae.

b) Difficulties with Magnetic Storage of Sunspot Blocked Energy

It has been suggested that the required long storage and re-radiation specifically from faculae might be explained if excess facular brightness is fueled by dissipation of magnetic energy representing sunspot blocked heat stored in magnetic flux tubes (Wilson 1981; Chapman 1984). But the magnetic energy of a flux tube is only increased if either the magnetic intensity or the volume of a flux tube increase in time, so only spots growing in area or in magnetic field strength should cause irradiance dips. This prediction does not appear compatible with the irradiance record which exhibits large dips whose time profiles follow changes in the projected area of spots. The true

area of these spots, measured to the accuracy of the NOAA-WDC records, is not in general found to change significantly during the time of the dip. The change in area or magnetic intensity required to store the energy of order 10^{36} ergs blocked during a large irradiance dip should be easily detectable (Foukal, 1981). Changes in magnetic energy stored at some depth might be invoked, but it seems difficult to understand how such deep changes in spot structure can occur on the short time scale of the irradiance dips while leaving the umbral area and field intensity relatively unaffected.

c) Similarity between Faculae and Network

Studies of photospheric flux tubes indicate that facular regions are similar in magnetic field intensity and atmospheric structure to the network flux tubes. The main difference seems to be that in facular areas, a larger number of flux tubes are packed together over a larger area than in the network (see, e.g., review by Zwaan 1981). Given this similarity, it seems reasonable that if the excess flux of faculae is to be derived from sunspot blocked flux, so should the excess flux of every network element on the sun, including polar faculae and quiet network. One might suppose that only magnetic elements around active regions derive their excess radiation from spots, while other mechanisms fuel the excess radiation of flux tubes in high latitudes and other distant quiet regions. However, this qualitative distinction seems contrived and has no observational support.

d) Topology of Spot and Facular Flux Tubes in Active Regions.

The concept of faculae as conduits of enhanced (nonthermal) flux also seems to encounter difficulties when we consider the topology of active region magnetic fields, as suggested by the types of observations that led to the conventional Babcock (1961) model of the solar activity cycle. Within this model, each bipolar active region is supposed to represent a Ω-shaped

stitch of magnetic flux connected to submerged fields on either side. If this picture is accepted, it is difficult to see how fluxes of, e.g., Alfven waves blocked by a spot could be channeled to a facula in the same active region unless it travels through the corona, which seems highly unlikely (Beckers and Schneeberger, 1977). One might envision such a redirected flux into a facular area in an adjoining active region in the same hemisphere. But in that case, we would expect to see a better correlation between the facular and sunspot brightness and area in adjacent active regions in the same hemisphere, than within the same region, where energy balance arguments have generally been applied.

One might depart from the Babcock model to form a U-shaped sub-photospheric connection between facula and spot within the same AR. But then it becomes difficult to understand why the Hale-Nicholson polarity laws should be so regularly obeyed, since each active region would constitute a self-contained loop disconnected from the sub-photospheric solar field.

VII. Discussion and Conclusions

The main result of this study is the finding that the solar irradiance records from the ACRIM and ERB radiometers, after subtraction of the calculated sunspot blocking contribution, exhibit a short-term modulation that is better explained by faculae than by errors in the sunspot blocking function, P_s.

This evidence is based on the 25% higher correlation coefficients found between the residuals $S-P_s$ and the facula-modulated 205 nm flux or the facular contribution function P_f, as compared to the correlation coefficient found with the P_s function itself. It is further based on the asymmetry of the

cross-correlation function of $S-P_s$ against P_s, in contrast to the symmetry found in the cross-correlation functions of $S-P_s$ against 205 nm flux or against P_f. This shows that the $S-P_s$ residuals are generated by solar structures whose lifetimes are typically at least 2 solar rotations, significantly greater than the typical lifetime of the spots observed between 1978-1982.

While the absence of a distinct peak at 28 days in the total irradiance power spectrum (actually, the presence of a local dip at this period) seems surprising given the very strong peaks at 28 days found in the power spectra of 205 nm, P_s, P_f and $S-P_s$, the most likely explanation is that the photometric contributions of spots and faculae are of roughly comparable magnitude, similar in phase and opposite in sign, thus causing cancellation of the two signals and reducing the amplitude of the 28-day power spectrum peak that is found in each separately. Lastly, we find that about 80% of the power in the residuals $S-P_s$ near 28 days is attributable to solar structures whose modulation of S follows the facula-generated 205 nm flux and P_f function, while only about 50% can be attributed to the sunspot-generated P_s function.

Taken together, these four lines of evidence indicate that faculae produce an important contribution to short-term modulation of the total solar irradiance. Similar results in cross-correlation and power spectrum analysis have recently been reported by Fröhlich (1984) although he did not identify faculae as the solar structures causing the additional modulation of irradiance beyond that of spots. The results found here from analysis of the space radiometry are also consistent with the finding of a significant cross-correlation (with recurrences at multiples of the solar rotation period) between facular areas and the APO ground-based radiometry (Foukal and Vernazza 1979).

Our calculation of the net contribution of spots and faculae to the irradiance during 1980 indicates that the facular contribution is comparable to

that of spots over time scales of active region evolution in that year. This result seems to be in agreement with the conclusions of Bruning and Labonte (1983), but in disagreement with those of Hoyt, Eddy, and Hudson (1983) who concluded that the facular contribution is small. These last authors did not specifically compare the time-integrated contributions of spots and faculae, so their conclusion applies to the relative modulation caused by spots and faculae, rather than to the time integrated contributions that require an accurate estimate of the quiet-sun irradiance. A definitive measurement of the relative facular and spot contributions should be possible from total irradiance data and projected areas of spots and faculae during the solar activity minimum period, since the main uncertainty in our result lies in the need to apply an uncertain correction for the facular contribution to the quiet sun irradiance on DOY77.

Several arguments we present on the storage time of energy in active regions, its dependence on spot evolution, and considerations of magnetic field-line geometry between faculae and spots lead us to conclude that faculae are unlikely to represent direct conduits for channeling and re-radiation of the missing sunspot radiative flux, even though such a detailed balance probably cannot be ruled out on energetic grounds alone. To us, the evidence seems to favor the view that faculae in active regions, polar areas and the general network represent local perturbations to photospheric heat flow that are physically independent of spots, of opposite sign (i.e., local heat leaks rather than thermal plugs) and of comparable magnitude. Reasonable physical models of such facular flux tubes and their effect as local photospheric heat leaks have been given by Zwaan (1965), Spruit (1976), Deinzer et al. (1984), and Chiang and Foukal (1984). Further progress on this topic would seem to require direct observational tests of such models using photometric, magnetic

and velocity measurements on faculae, rather than relying mostly on studies of the global energy balance between spots and faculae, which have been emphasized so far.

We are grateful to R. Willson, J. Hickey, and D. Heath for providing solar irradiance data analyzed in this paper. We also thank T. Repoff of NOAA-ARL for allowing us to use his statistical analysis routines, and for discussions on their interpretation. This work was supported at AER, Inc. under NSF grant ATM 8401480 and NASA contract NAS W4062.

References

Babcock, H., 1961. Ap. J., 133, 572.

Beckers, J. and Schneeberger, T., 1977. Ap. J., 215, 356.

Bruning, D., and Labonte, B., 1983. Ap. J., 271, 853.

Chapman, G., 1980. Ap. J. (Letters), 242, 45.

Chapman, G., 1984. Nature, 308, 252.

Chiang, W.-H., and Foukal, P., 1984. Solar Phys. (in press).

Deinzer, W., Hensler, G., Schüssler, M., and Weisshaar, E. 1984, Astr. Ap., 139, 435.

Foukal, P., 1981. In Physics of Sunspots, L. Cram and J. Thomas (eds.), SPO publication, p. 391.

Foukal, P., and Vernazza, J., 1979. Ap. J., 234, 707.

Fröhlich, C., 1984, preprint.

Fröhlich, C., and Eddy, J. A., 1984. Paper presented at COSPAR, July 1984 Session E-2, Graz, Austria.

Heath, D., 1980. In "Sun and Climate," R. Kandel (ed.), CNRS publication, p. 447.

Heath, D., Repoff, T., and Donnelly, R., 1984. NOAA Technical Memorandum ERL ARL-129.

Hickey, J., Griffin, F., Jacobwitz, H., Stowe, L., Pellegrino, P., and Maschhoff, R., 1980. EOS, 61, 355.

Hoyt, D., and J. Eddy, 1982. NCAR Technical Note TN-194 + STR.

Hoyt, D., Eddy, J., and Hudson, H., 1983. Ap. J., 275, 878.

Hudson, H., and R. Willson, 1981. In Physics of Sunspots, L. Cram and J. Thomas, eds. SPO publication, p. 434.

Kiepenheuer, K., 1953. In The Solar System, Vol I, The Sun, G. Kuiper, ed. (Univ. of Chicago Press) p. 322.

Lean, J. L., White, O. R., Livingston, W. C., Heath, D. F., Donnelly, R. F., and Skumanich, A., 1982. J. Geophys. Res., 87, 10307.

Oster, L., Schatten, K., and Sofia, S., 1982. Ap. J., 256, 768.

Spruit, H., 1976. Solar Physics, 50, 269.

Vernazza, J., Avrett, E., and Loeser, R., 1981. Ap. J. Suppl., 45, No. 4

Willson, R. C., Gulkis, S., Janssen, M., Hudson, H. S., and Chapman, G. A., 1981. Science, 211, 700.

Wilson, P., 1981. In "The Physics of Sunspots," L. Cram and J. Thomas (Eds.), SPO Publications, p. 391.

Zwaan, C., 1965. Rech. Astron. Obs. Ulrecht, 17, part 4.

Zwaan, C., 1981. In "The Sun as Star," S. Jordan (Ed.), NASA Publications, SP450, p. 163.

Table 1

The Net Contribution of Sunspots and Faculae to S,

Calculated from Equation (5)

t_2-t_1 (t_1 = DOY47)	$2.5\times10^{-4}(t_2-t_1)$ (% of S_{max})	$\int_{t_1}^{t_2} S'dt$ (% of S_{max})	$\int_{t_1}^{t_2} \left(\frac{\Delta S_s+\Delta S_f}{S_{max}}\right)dt$ (% of S_{max})
50	1.25	2.00	-0.75
100	2.50	5.48	-2.98
150	3.75	8.49	-4.74
200	5.00	11.44	-6.44
250	6.00	14.85	-8.85

Figure Captions

Fig. 1. Simultaneous daily measurements of the total solar irradiance in 1980 from a) the ACRIM radiometer on the Solar Maximum Mission and b) the ERB radiometer on the Nimbus-7 satellite. The data have been detrended with a 12th order polynomial and plotted about the mean value for the five-year period. The points marked A and B refer respectively to values measured on DOY 77 and DOY 110 (see text).

Fig. 2. Plots of daily values for 1980 of a) the P_S function, b) the residuals ACRIM - P_S, c) the 205 nm ultraviolet flux, and d) the calculated facular contribution to S, the P_f function. Detrended data plotted about the five-year mean value.

Fig. 3. Plots of the full data sets (1978-1982) used in this study for a) the ACRIM - P_S residuals, b) the ERB - P_S residuals, c) the sunspot blocking function P_S (plotted with reversed sign to facilitate comparison with the peaks of ACRIM - P_S and ERB - P_S), d) the calculated facular irradiance contribution P_f, and e) the 205 nm ultraviolet flux. Detrended and plotted about the five-year mean.

Fig. 4. Cross-correlation functions (solid lines) of ACRIM - P_S vs. a) - P_S, b) 205 nm flux, and c) P_f, and ERB - P_S vs. d) - P_S, e) 205 nm, and f) P_f. The dashed lines in a) and d) give the autocorrelation functions of ACRIM _ P_S and ERB - P_S, respectively.

Fig. 5. Normalized power spectra of a) the detrended ACRIM radiometry 1980-1982, b) the detrended ERB radiometry 1978-1982, c) the 205 nm ultraviolet flux, d) the (sign reversed) sunspot blocking function $-P_S$, e) the ACRIM $-P_S$ residuals, and f) the calculated facular irradiance contribution P_f. The ordinate is in percent of integrated power.

Fig. 6. Power spectra of the ACRIM $-P_S$ residuals (a, b, c) and ERB $-P_S$ residuals (d, e, f) plotted on solid lines together with (dashed lines) the power explained as a function of period by the variations in $-P_S$, in 205 nm flux, and in P_f.

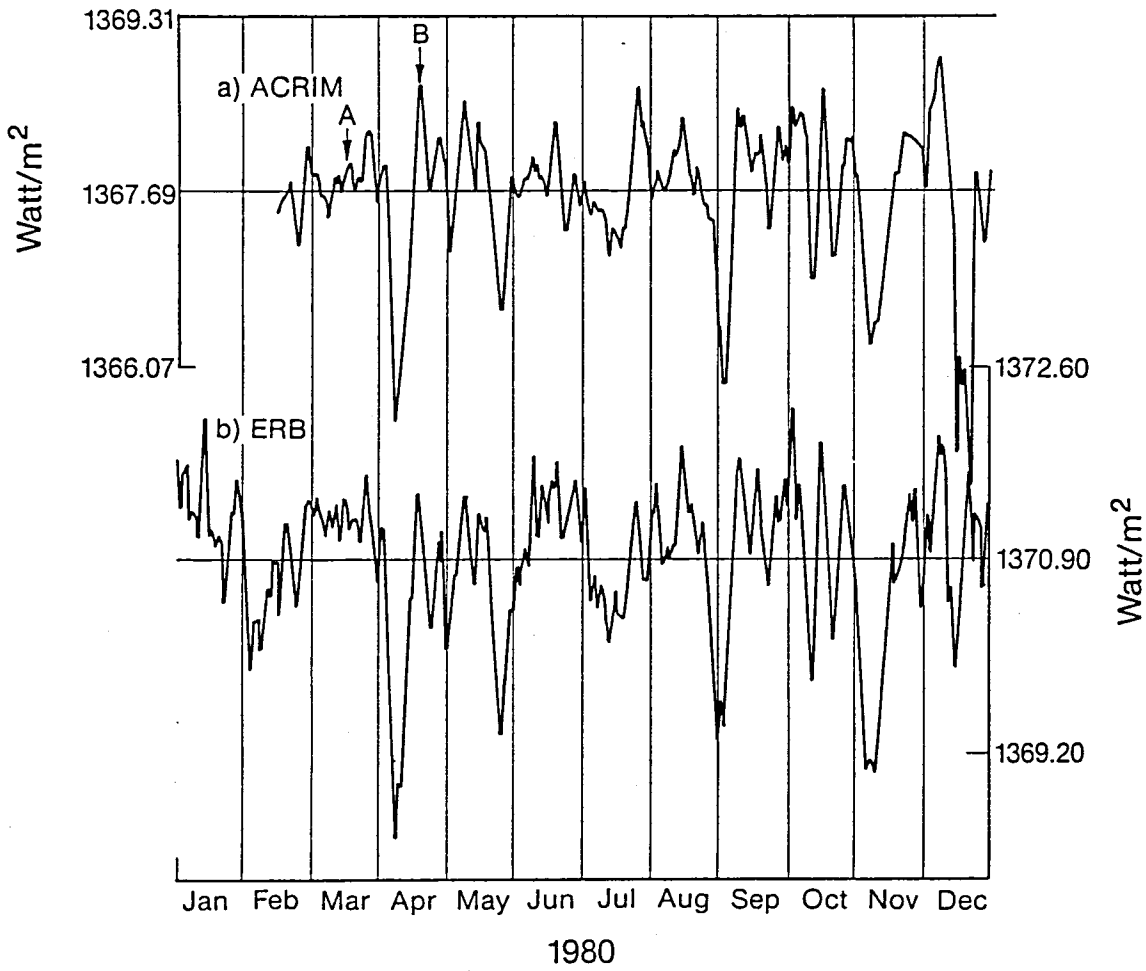
1369.31
B
a) ACRIM
A
1367.69
1366.07
1372.60
b) ERB
1370.90
1369.20
Watt/m2
Watt/m2
Jan
Feb
Mar
Apr
May
Jun
Jul
Aug
Sep
Oct
Nov
Dec
1980

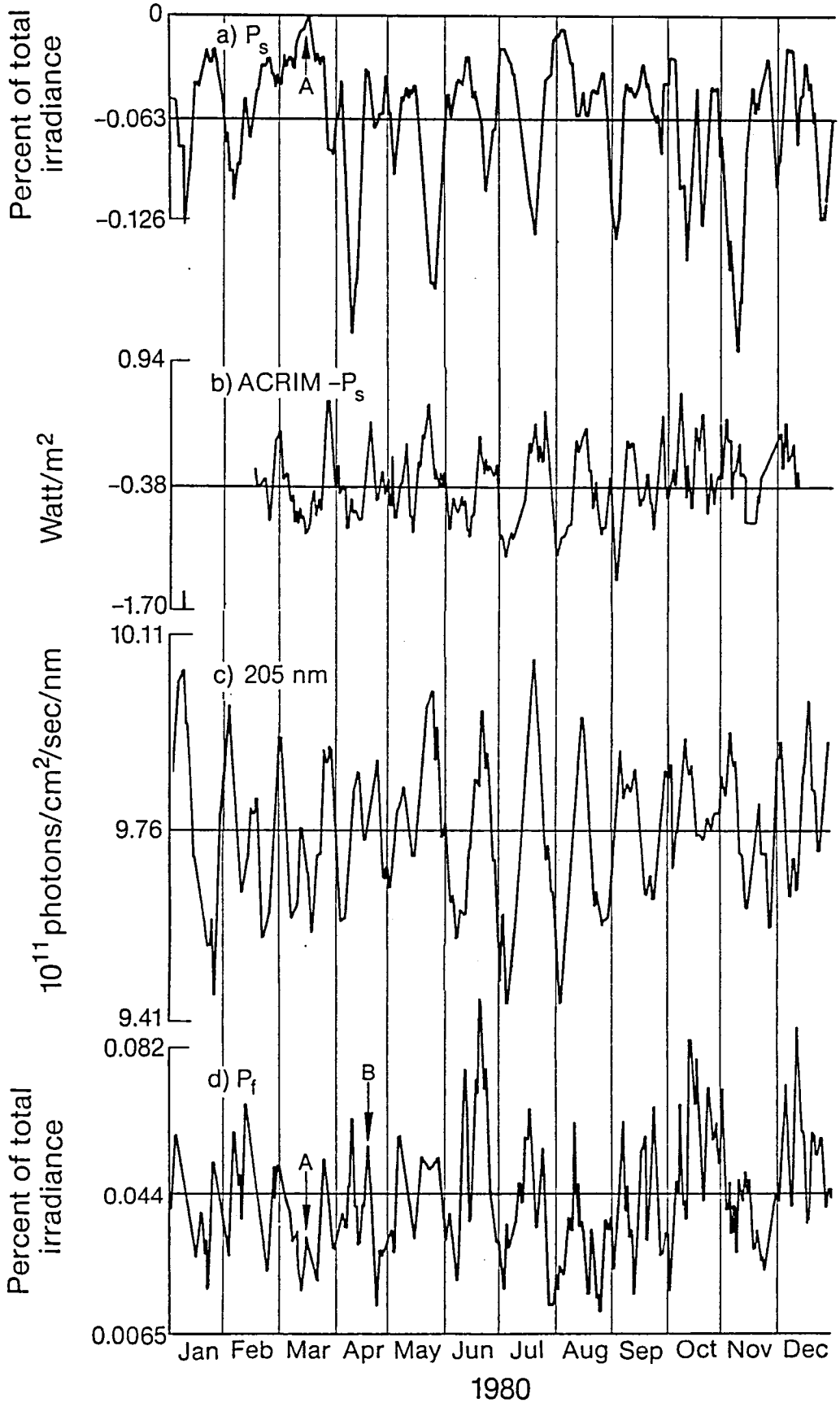
Percent of total irradiance
0
a) P_s
A
-0.063
-0.126
0.94
b) ACRIM -P_s
Watt/m^2
-0.38
-1.70
10.11
c) 205 nm
10^{11} photons/cm^2/sec/nm
9.76
9.41
0.082
d) P_f
B
A
Percent of total irradiance
0.044
0.0065
Jan Feb Mar Apr May Jun Jul Aug Sep Oct Nov Dec
1980

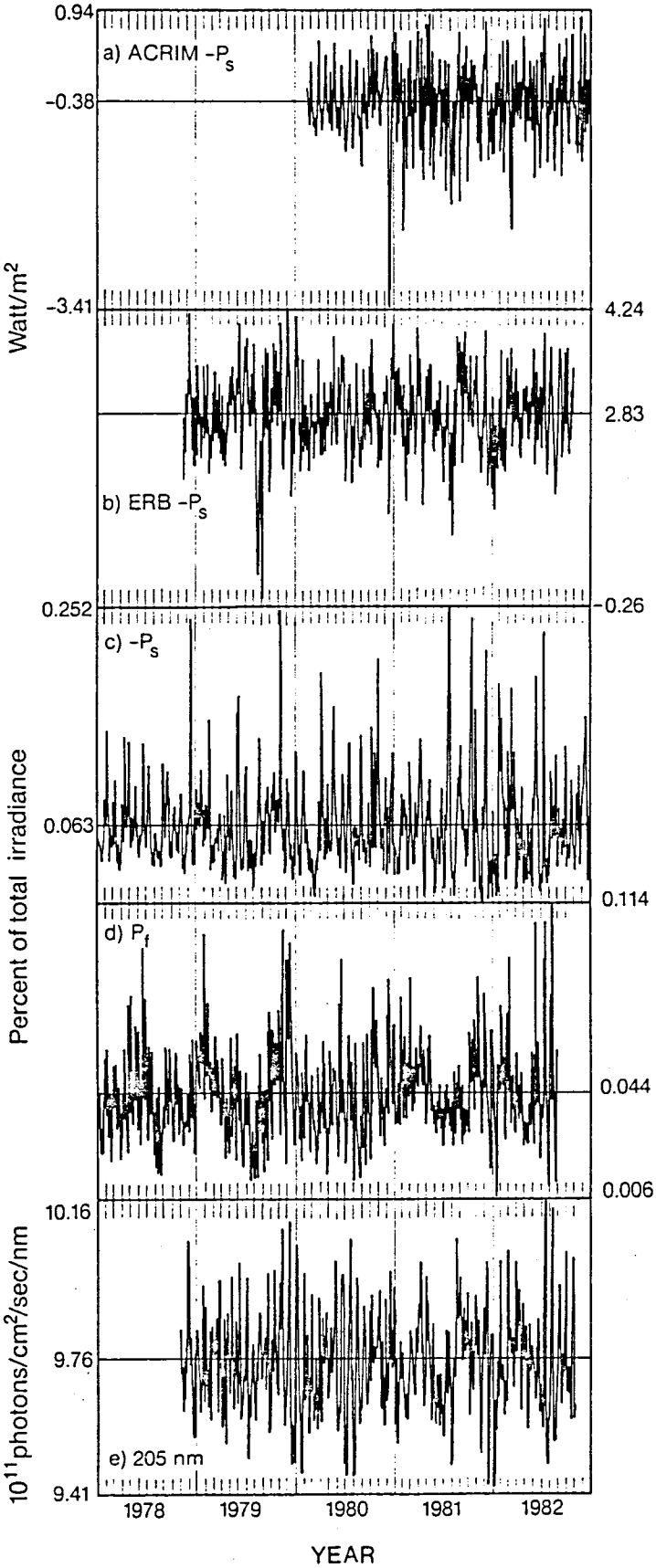
0.94
a) ACRIM -P_s
-0.38
-3.41
4.24
2.83
b) ERB -P_s
0.252
-0.26
c) -P_s
0.063
0.114
d) P_f
0.044
0.006
10.16
9.76
e) 205 nm
9.41
Watt/m^2
Percent of total irradiance
10^{11}photons/cm^2/sec/nm
1978
1979
1980
1981
1982
YEAR

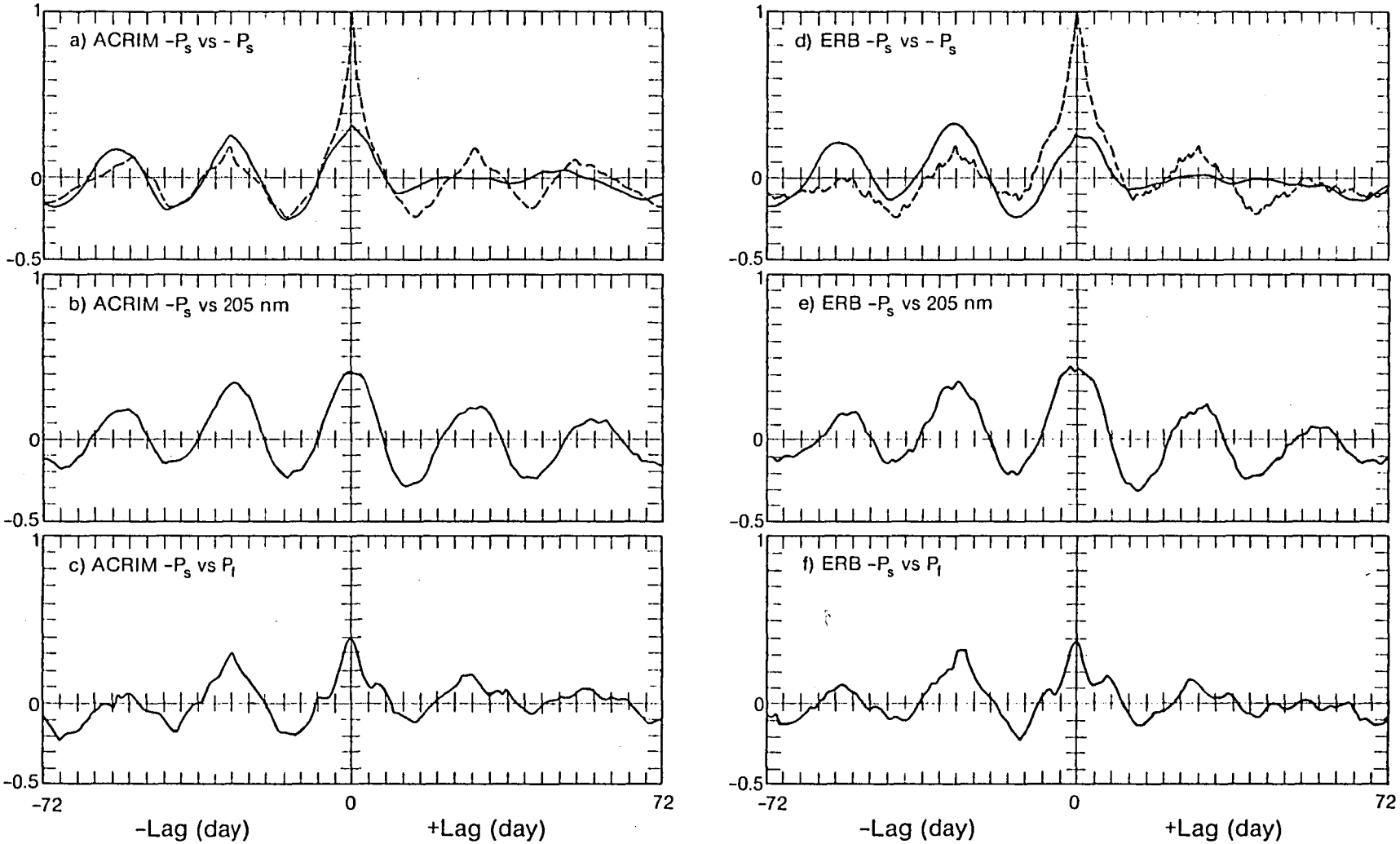
a) ACRIM -P_s vs - P_s
b) ACRIM -P_s vs 205 nm
c) ACRIM -P_s vs P_f
d) ERB -P_s vs - P_s
e) ERB -P_s vs 205 nm
f) ERB -P_s vs P_f
1
0
-0.5
-72
0
72
-Lag (day)
+Lag (day)

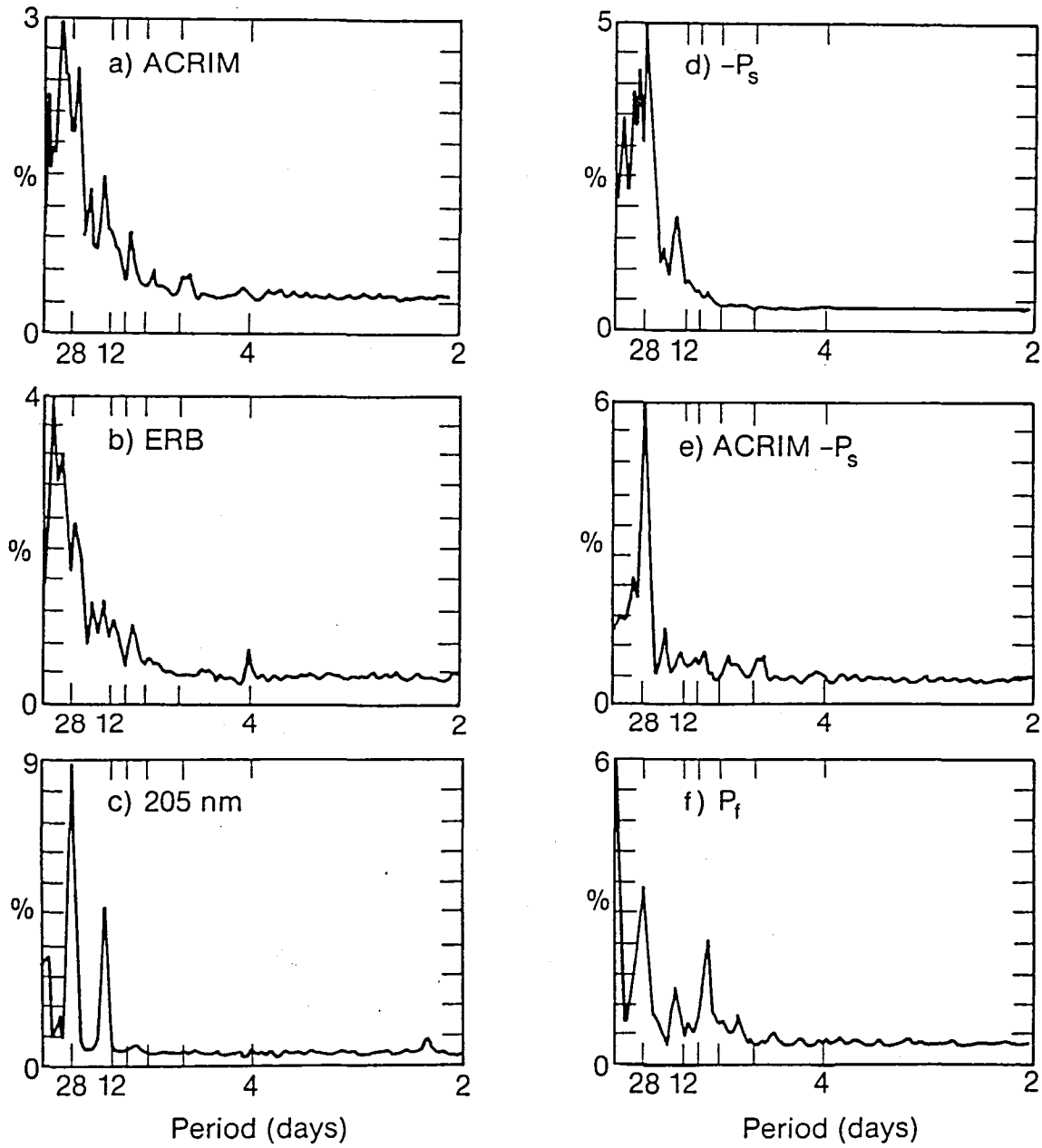
a) ACRIM
b) ERB
c) 205 nm
d) -Ps
e) ACRIM -Ps
f) Pf
%
3
0
4
9
5
6
28 12
4
2
Period (days)

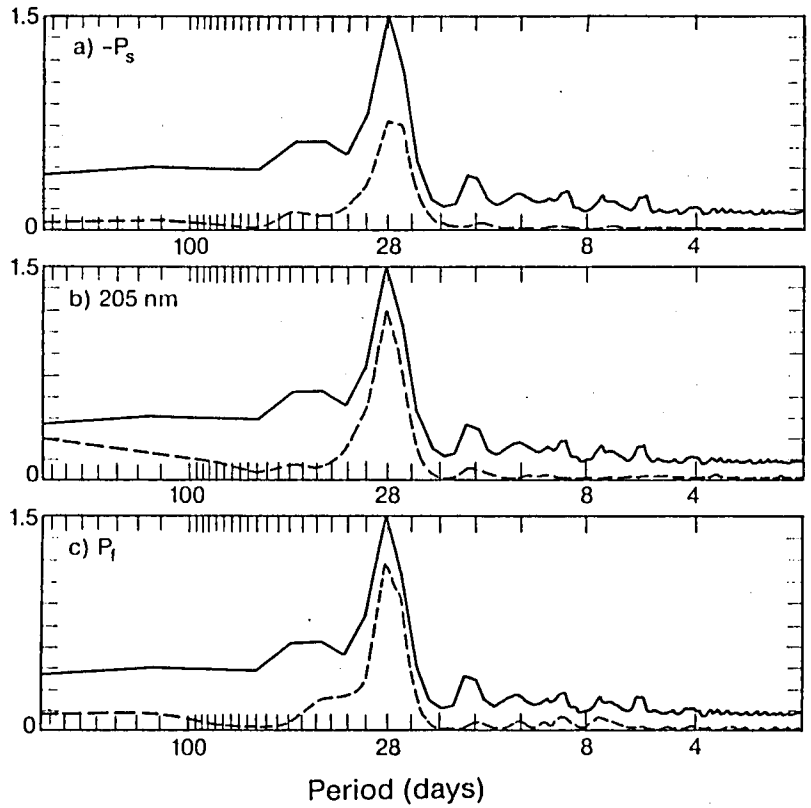
1.5
a) -P_s
0
100
28
8
4
1.5
b) 205 nm
0
100
28
8
4
1.5
c) P_f
0
100
28
8
4
Period (days)

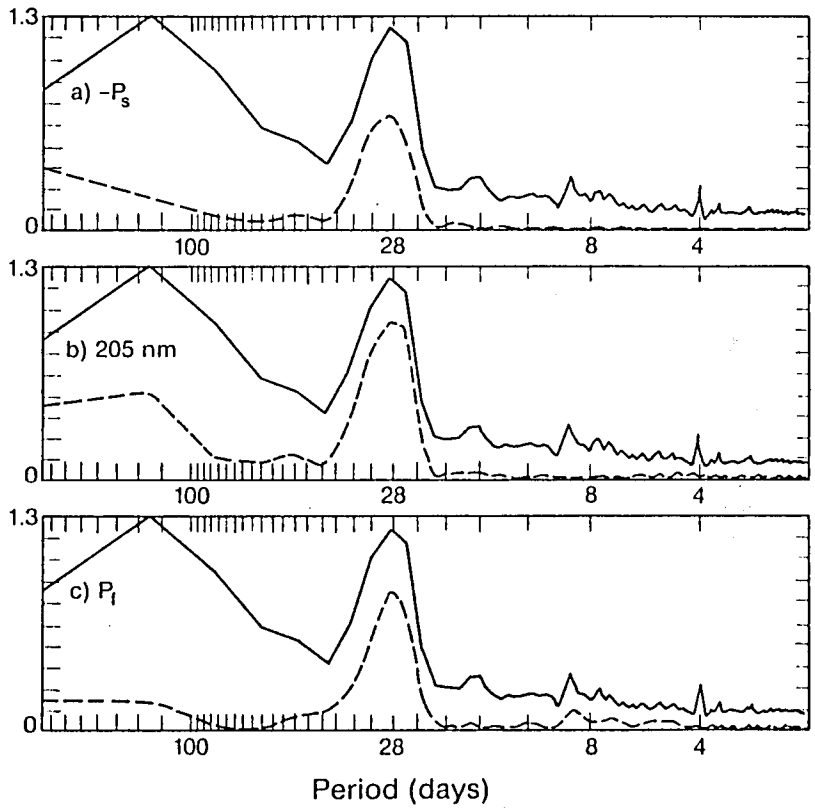
1.3
a) -P_s
0
100
28
8
4
1.3
b) 205 nm
0
100
28
8
4
1.3
c) P_f
0
100
28
8
4
Period (days)

APPENDIX C

Physical Interpretation of Variations in Total Solar Irradiance

P. Foukal

Cambridge Research and Instrumentation, Inc.

Cambridge, Massachusetts 02139

Invited Review Presented at the American Geophysical Union Meeting in San Francisco, December 13, 1985.

Submitted to the Journal of Geophysical Research Special Collection on Solar Variability

Abstract

Radiometry from the Solar Maximum Mission and Nimbus-7 satellites has demonstrated that the solar constant varies at a peak-to-peak level of up to 0.2% on time scales of weeks. The rotation and evolution of dark spots and bright faculae across the sun's disc accounts for most of that variation. Reasonable explanations have been put forward to explain how the spot-blocked heat flow might be stored, and to explain the source of the intense radiation that gives rise to the increased irradiance produced by the bright magnetic faculae. Time-dependent models of the solar convection zone's response to small perturbations also indicate that slower variations in S of comparable magnitude are likely. More precise observations of the total solar irradiance and radius over long time scales are required to demonstrate the existence of such climatologically relevant changes and to test models that would enable us to interpret and possibly predict them.

1. Introduction

For the purposes of climate studies, one would like to have measurements of the power spectrum of total solar irradiance, S, over the time scales of roughly 10^6 secs or more that might directly influence the tropospheric energy balance. More rapid variations of the sun's total output are less likely to provide a direct influence, although such higher frequency couplings through, e.g., forcing of planetary waves (Volland 1979) have also been suggested.

Radiometry from balloons, rockets, and satellites over the past 20 years (see reviews by Foukal 1980, Frohlich 1981, Willson 1984) support the earlier results of ground-based measurements (Abbot 1952, Sterne and Dieter 1958) in showing that any slow variations in S must be below the 0.5% level over decades. But the direct measurement of slow variations in S that may be present at or below the level of a few tenths of a percent has proven elusive, given the difficulties found in maintaining very precise calibrations with even the best space-borne radiometers (Willson 1985, Hickey et al. 1985).

These radiometers have, however, demonstrated conclusively that S varies at a level up to 0.2% over times scales of days to weeks (Willson et al. 1981, Hickey et al. 1980). The fluctuations recorded during 1980 by the ACRIM radiometer on the Solar Maximum Mission and the ERB radiometer on Nimbus-7 are shown in Figure 1. The dominant contribution to these variations arises from the influences of magnetic sunspots and faculae on the flow of energy to the photosphere.

Hoyt and Eddy (1982) have shown that the 11-year variation of spot area over the solar cycle is insufficient in itself to produce even a 0.1% peak-to-peak variation in S. However, study of these relatively short-term irradiance fluctuations gives us an opportunity to learn more about the interaction of solar convection with magnetic fields. This interaction is likely to also play a prominent role in driving slower variations in S that could influence climate on human time scales.

In this review we discuss what is known about the sunspot effect on solar luminosity, in section 2, and our understanding of the facular influence, in section 3. In section 4 we discuss the physical nature of spots and faculae as regards their influence on photospheric heat flow. A brief discussion of possible mechanisms that might produce slow variations in luminosity over years is given in section 5. In section 6 we summarize our present understanding.

2. Sunspot Influence on Total Solar Irradiance

Figure 2 shows a portion of the ACRIM irradiance record along with a plot of the function P_s which describes variations of S expected if dark spots were to reduce solar radiative output in exact proportion to their wide-band photometric contrast and projected area. We see that the timing and to a lesser extent the amplitude of the larger dips in S correlate well with the major dips predicted in P_s.

The requirement that the sun's output be reduced by a factor approximately given by the product of the spot's

projected area and its contrast poses an important constraint on the mechanism responsible for the luminosity reduction. A further constraint is provided by the fact that an irradiance dip of amplitude 0.2% lasting about ten days represents storage of approximately 10^{36} ergs.

It has been suggested that the mechanical work done by convection in building up the spot's field might lead to storage of the missing luminosity in the spot's magnetic energy (Wilson 1981, Chapman 1984). But it is difficult to see why the work $\int B^2/8\pi \, dV$ performed in intensifying the field should resemble the product of the spot's projected area and photometric contrast. In particular, the above integral only increases while a spot's volume and/or magnetic intensity are growing. We would thus expect only growing spots to cause dips in S. In fact, comparisons of P_s with the ACRIM data indicate that large, stable, or decaying spots are mainly responsible for the large irradiance dips.

More generally, in the absence of a good theory of how spots are formed, it actually remains unclear whether the process of formation of large-diameter, intense flux tubes is likely to withdraw energy from convection or dump excess energy into it, given the flux tube's reservoirs of magnetic and potential energy along with with the thermal and kinetic energy reservoirs available to the convection.

The idea that the spot's missing energy resides in downdrafts (Schatten 1984) seems to require downflow velocities that lie well outside the errors of about 10 $msec^{-1}$ in

absolute velocity measurements made in umbrae by Beckers (1977).

A simple model that does seem to explain the available evidence represents the spot as a thermal plug which locally prevents most of the convective heat flux from reaching the photosphere. How this inhibition occurs is of little importance. The essential point is that the radiative flux from the spot is lowered by a certain factor.

Suppose now that such a thermal plug is inserted at the photosphere of an equilibrium solar convection zone, at time $t = t_o$. At $t < t_o$, the radiative flux into the convective zone from the deeper layers of the solar interior equals the radiative flux $F = \sigma T^4 A$ at the upper boundary, from the photosphere of temperature T and area A. At $t = t_o$ the radiative flux from the photosphere will be reduced by the exact factor $(C_s - 1)A_s/A$ where $C_s = I_s/I_{ph}$ is the wide-band photometric contrast of the spot, and A_s is the spot's projected area. For $t > t_o$, the convection zone outside the spot will heat up until $F = \sigma T'^4 A'$ where $T' > T$ since $A' < A$ (due to the photospheric area occupied by the spot).

If this heating from T to T' took place instantly, we would expect to see no effect of spots on L_o. If we represent solar convection in this model as a process of eddy diffusion with a radiative upper boundary (Foukal 1981, Spruit 1981), we find that heating of the photosphere is actually remarkably slow, due to the large thermal inertia. Figure 3 shows the

isotherm perturbations caused in such a model by insertion of a spot.

The actual equilibration time scale is as uncertain as our limited understanding of the most efficient modes of solar convection. It might be as long as 10^5 years, the time scale for radiative relaxation of the full convection zone depth. Improved understanding on this problem will require use of a dynamical simulation of convection to replace the eddy diffusion representation.

The main point is that the relaxation time is likely to be much longer than the typical ten-day duration of the observed dips, or even than the spot's lifetime. In that case, the luminosity reduction will continue to be equal to $(C_s - 1)A_s$ over the spot's lifetime. It makes no difference whether the spot is growing or decaying. Also, the total amount of energy to be stored presents no problem since storage occurs in the slightly heated (and expanded) convection zone outside the spot.

3. Faculae Influence on the Total Solar Irradiance

The residuals $S - P_s$ found after the spot-blocking function $-P_s$ is removed from the observed irradiance time series are shown in Figure 4, along with the 205 nm ultraviolet flux. It is easy to see that while spots explain a substantial component of the variance in S, a remaining component exists that correlates very well with modulation of the sun's ultraviolet continuum flux.

It has been shown that the ultraviolet modulation arises mainly from the evolution and rotation of magnetic faculae across the sun's disc. Since the faculae are also known to be brighter than the photosphere in the visible, it is likely that the residuals $S - P_s$ can be explained as the influence of faculae on the total solar irradiance.

A detailed study of the facular influence on S was carried out recently by Foukal and Lean (1985). It was found that to within uncertainties in defining a truly "quiet" solar constant, the facular contribution to S was at least comparable to that of spots, when integrated over months. This result, based on wide-band space-borne radiometry is consistent with ground-based photometric measurements made in visible light of spots and faculae (e.g., Chapman 1980, Lawrence et al. 1985), which also indicate that the missing radiative flux of dark spots and the excess radiative flux of bright faculae seem roughly comparable to 30-50%. If the spot and facular contributions could be shown to compensate to within a few percent, an argument might be made for some kind of detailed balancing of energy within a given active region. But the error bars are too large to make a convincing argument based on energy balance alone.

The observation that the angular dependence of the facular radiation field is more heavily weighted toward angles far from the local normal means that the relative contributions to S of spots and faculae will depend on their coordinates on the disc (Oster et al. 1982). Consequently, we would not expect

their contributions to cancel at any given disc position, even if their total radiative flux contributions (integrated over angle) did exactly compensate.

4. The Physical Nature of Faculae and Spots

The physical model of faculae that seems to best explain their photometric appearance and magnetic properties is sketched in Figure 5. One of its attractive aspects is its ability to explain why large-diameter solar magnetic flux tubes (i.e., sunspots) appear dark, while photospheric areas of similar (kilogauss-level) magnetic intensity, but consisting of smaller-diameter flux tubes, produce the bright areas called faculae.

This model indicates that when a magnetic field is confined to a slender vertical flux tube, magnetohydrostatic equilibrium requires a lower internal gas pressure and thus also a lower opacity than in the surrounding photosphere. This lower opacity enables us to see to a greater geometrical depth inside the flux tube, resulting in a local geometrical depression of a few hundred kilometers of the iso-optical depth contours. This effect is referred to as the Wilson depression, in honor of Alexander Wilson, a Glasgow University professor, who discovered it in 1774, from the changing geometry of sunspots that he observed rotating across the limb.

For both faculae and spots, the energy inputs that determine the temperature structure in the flux tube atmosphere around $\tau_{0.5} = 1$ are dominated by the rate of convective energy flow along the flux tube axis (assumed to be reduced below

photospheric values, for both spots and faculae) and by the flux of radiation from the wall of the Wilson depression. This radiation field is more intense than photospheric radiation because it emerges from deeper, hotter layers than those that are seen in non-magnetic regions in white light.

The key distinction between dark spots and bright faculae can then be explained strictly as a matter of size, since radiative heating of the flux tube interior at levels above $\tau_{0.5} = 1$ becomes more important relative to the axial transport, as the flux tube diameter decreases. This is simply because the ratio of hot wall area to flux-tube cross-sectional area increases. For sunspot flux tubes the reduction of axial heat flow then dominates and we see a dark structure. In faculae, the field is known to consist of more slender flux tubes, as can be seen from Figure 6, where the facular regions are resolved into many small bright dots. The radiative heating in such small structures more than overcomes the reduction of axial convection and we see a structure whose brightness temperature exceeds that of the photosphere.

Several studies have treated this basic model (Zwaan 1965, Spruit 1976, Deinzer et al. 1984, Ferrari et al. 1985), using various degrees of sophistication in their treatment of the radiative transfer problem, and they vary in their predictions on the facular photometric contrast and its disc center-to-limb behavior. Since observational uncertainties are also quite large (Chapman 1977, 1979), the main virtue of the model is the simple explanation it provides for at least

the qualitative aspects of magnetic activity influence on heat flow near the photosphere.

It would be attractive to explain why the facular and spot perturbations are in fact similar in magnitude, since the arguments given above make no predictions on that score. Unfortunately, the dynamical interaction of magnetic fields and solar convections is not well enough understood to calculate the fractional reduction of axial convective transport--this is an adjustable parameter in these thermal models.

Chapman (1984) has suggested that faculae are heated by ohmic dissipation of sunspot magnetic flux tubes. If true, this would explain why sunspot and facular contributions to the luminosity are comparable. But this explanation requires further that sunspot-blocked heat is stored magnetically in spots to obtain the desired balance of radiative fluxes. This magnetic storage in spot fields seems to be on weak grounds for the reasons given above in section 2.

There are also some general arguments against energetic balance between spots and faculae that have been expounded recently by Foukal and Lean (1985). For one, it seems unlikely that every bright facular element on the sun, including those in the globally distributed magnetic network, is heated by virtue of being connected subphotospherically to a spot. Yet the current belief (e.g., Zwaan 1981) is that facular and network magnetic flux tubes are thermodynamically similar, differing mainly in diameter. Second, it is difficult to see how energy could be transported from spots to faculae without

using the active region field geometry to guide it in the form of waves, or mass flows. This connection must occur subphotospherically, for it is energetically implausible that the huge fluxes required should travel through the corona. But the geometry of the AR field derived from the observations on which the Babcock dynamo model of the solar activity cycle is based, requires that the magnetic connection between faculae and spots in a given active region be made above the photosphere (see Figure 7). For these and other reasons, it seems unlikely that a detailed energy balance holds between spots and faculae.

5. Theoretical Studies of ΔL_o over Time Scales of Years

Recent investigations of possible slow changes in the solar diameter have led to increased theoretical study of the time-dependent behavior of the sun's radius and luminosity. The most complete studies (Gilliland 1981, Endal and Twigg 1982) show that one must be careful to base such investigations on integrations of the full set of non-linearly coupled equations describing mass, momentum and energy conservation in the solar interior. Earlier studies which focused on only the dynamical effect of changing magnetic pressure inside the convection zone over the 11-year cycle, or alternatively only its influence on convective heat transport, have been shown to be misleading in both the sign and magnitude of the predicted effects on L_o and R_o.

It now appears that the models used are at least consistent in their predictions of the variability of L_o and R_o for

a given change in the efficiency of solar convection, at a given depth. They seem to agree in estimating that the fractional variation in radius should be three to four orders of magnitude smaller (immediately after a perturbation) than the fractional change in L_o. Typical variations in L_o and R_o caused by a 22-year periodic variation in the convective efficiency parameter α of mixing length models are illustrated in Figure 8.

Unfortunately, our understanding of what perturbations to convective efficiency to expect below the photospheric layers is still very sketchy. These models suggest that α-variations of 0.2% could cause detectable (and probably climatologically significant) changes in L_o and S. Such α-variations might be detected through studies of the frequency variation of p-mode oscillations of around 5 minutes period, over the solar cycle. Some evidence for such a frequency variation has been reported from analysis of photospheric p-mode brightness oscillations detected in the ACRIM radiometry (Woodard and Noyes 1985).

6. Summary

The most important findings are:

i) Total solar irradiance fluctuations on time scales of days and weeks are caused by the evolution of spots and faculae and their rotation across the photospheric disc.

ii) The most plausible explanation of a spot's influence on total irradiance indicates that the heat flux blocked by the dark spot is stored in the slightly increased internal and potential energy of the sun's convective layers. More

stringent tests will require dynamical modeling of the interaction of solar convection with intense magnetic flux tubes.

iii) The excess radiation of faculae, and thus their tendency to compensate the spot-induced reduction of L_o seems to be best explained as a consequence of radiative heating of the facular atmosphere. Non-thermal heating of faculae by wave or electric current dissipation cannot be ruled out, but observational support for a direct energetic connection between spots and faculae within a given active region is weak. Observations of the relative importance of spots and faculae on other late-type stars might provide some important clues here.

iv) Variations in convective efficiency of a spontaneous, self-excited nature, or driven by a magnetic influence are quite likely to cause slow changes in S of climatological interest. However, our theoretical understanding of solar magneto-convection is still too rudimentary to attempt a prediction of the sign or magnitude of the variations to be expected over a solar magnetic cycle.

This work was supported at CRI, Inc., under NASA contract NASW4062 and NSF grant ATM 8408224, subcontracted through AER, Inc.

References

Abbot, C., 1952, Astrophys. Obs. Smithsonian Inst. Ann., 7, 165.

Beckers, J., 1977, Ap. J. 213, 900.

Chapman, G., 1977, Ap. J. Suppl. 33, 35.

Chapman, G., 1979, Ap. J. 232, 923.

Chapman, G., 1980, Ap. J. (Letters) 242, 45.

Chapman, G., 1984, Nature, 308, 252.

Deinzer, W., Hensler, G., Schussler, M., and Weisshaar, E., 1984, Astr. Ap. 139, 435.

Endal, A., and Twigg, L., 1982, Ap. J. 260, 342.

Ferrari, A., Massaglia, S., Kalkofen, W., Rosner, R., and Bodo G., 1985, Ap. J. 298, 181.

Foukal, P., 1980, in "The Ancient Sun," R. Pepin, J. Eddy and R. Merrill, eds., Pergamon Press, p. 29.

Foukal, P., 1981, in "The Physics of Sunspots," L. Cram and J. Thomas, eds., Sacramento Peak Observatory Publication, p. 391.

Foukal, P., and Lean, J., 1986, Ap. J., in press (March 15, 1986, issue).

Frohlich, C., 1981, in "Variations of the Solar Constant," S. Sofia, ed., NASA Conference Publication 2191.

Gilliland, R., 1981, Ap. J., 248, 1144.

Hickey, J., 1985, in "Advances in Absolute Radiometry," P. Foukal, ed., p.6 (Proceedings of a conference available from CRI, Inc., Cambridge, MA, 02139).

Hoyt, D. and Eddy, J., 1982, NCAR Tech Note TN-194 + STR.

Lawrence, J., Chapman, G., Hertzog, A., and Shelton, J., 1985, Ap. J. 292, 297.

McIntosh, P., and Wilson, P., 1985, Solar Phys. 97, 59.

Oster, L., Schatten, K., and Sofia, S., 1982, Ap. J. 256, 768.

Schatten, K., 1984, in "Solar Irradiance Variations on Active Region Time Scales," B. Labonte et al. eds., pp. 125 and 145.

Spruit, H., 1976, Solar Physics 50, 269.

Spruit, H., 1981, in "The Physics of Sunspots," L. Cram and J. Thomas, eds. Sacramento Peak Observatory Publication, p. 391.

Sterne, T., and Dieter, N., 1958, Smithsonian Contr. Ap., 9, 3.

Volland, H., 1979, in "Solar-Terrestrial Influences on Weather and Climate," B. McCormac and T. Seliga, eds., D. Reidel Publishing, p. 263.

Willson, R., 1985, in "Advances in Absolute Radiometry," P. Foukal, ed. p. 6 (Proceedings of a conference available from CRI, Inc., Cambridge, MA 02139).

Willson, R., Gulkis, S., Johnson, J., Hudson, H., and Chapman, G., 1981, Science 211, 700.

Willson, R., 1984, in "Solar Irradiance Variations on Active Region Time Scales," B. Labonte et al. eds. NASA Conference Publication 2310.

Wilson, P., 1981, in "The Physics of Sunspots," L. Cram and J. Thomas, eds. Sacramento Peak Observatory Publication, p. 83.

Woodard, M., and Noyes, R., 1985, Nature, 318, 449.

Zwaan, C., 1965, Rech. Astron. Observ. Utrecht 17, part 4.

Zwaan, C., 1981, in "The Sun as a Star," S. Jordan, ed. NASA Publications SP450, p. 163.

Figure Captions

Fig. 1 Plots of total solar irradiance values measured simultaneously with the ACRIM radiometer on the Solar Maximum Mission and the ERB radiometer on Nimbus-7 (from Foukal and Lean 1986)

Fig. 2 Plots of ACRIM irradiance values and of irradiance variations calculated using the sunspot-blocking function P_s calculated by Hoyt and Eddy (1982)

Fig. 3 Isotherms (of superadiabatic temperature) in the convective zone around a spot (rectangle at upper left). Isotherms at $t < t_o$, before the spot is "turned on," are shown in the left panel. Right panel shows perturbed isotherms at $t > t_o$.

Fig. 4 Residuals of S P_s plotted together with the function P_s, the 205 nm ultraviolet flux (measured on Nimbus-7 by D. Heath) and a function P_f estimating the facular contribution to S, based on facular areas and white light contrast values (from Foukal and Lean 1986).

Fig. 5 Schematic diagram of a facula and its temperature structure. The left-hand panel illustrates the magnetic field geometry passing through the photosphere, and the Wilson depression. The temperatures T_3, T_2, and T_1 in the right-hand panel refer respectively to the brightness temperatures of the bottom of the Wilson depression, its hot walls, and the undisturbed photosphere.

Fig. 6 Continuum light photoheliogram of dark spots and bright faculae near the limb.

Fig. 7. Schematic diagram of the magnetic field geometry (solid line) connecting a spot and a facula through the corona within an active region. The dashed line indicates the subphotospheric connection required to transport sunspot missing energy to faculae in the same active region.

Fig. 8. Plots of the fractional variations in radius $\Delta R_\odot/R_\odot$ and in luminosity $\Delta L_\odot/L_\odot$ expected from a 22-year variation in the convective efficiency parameter $\Delta\alpha/\alpha$ (adapted from Endal and Twigg 1982).

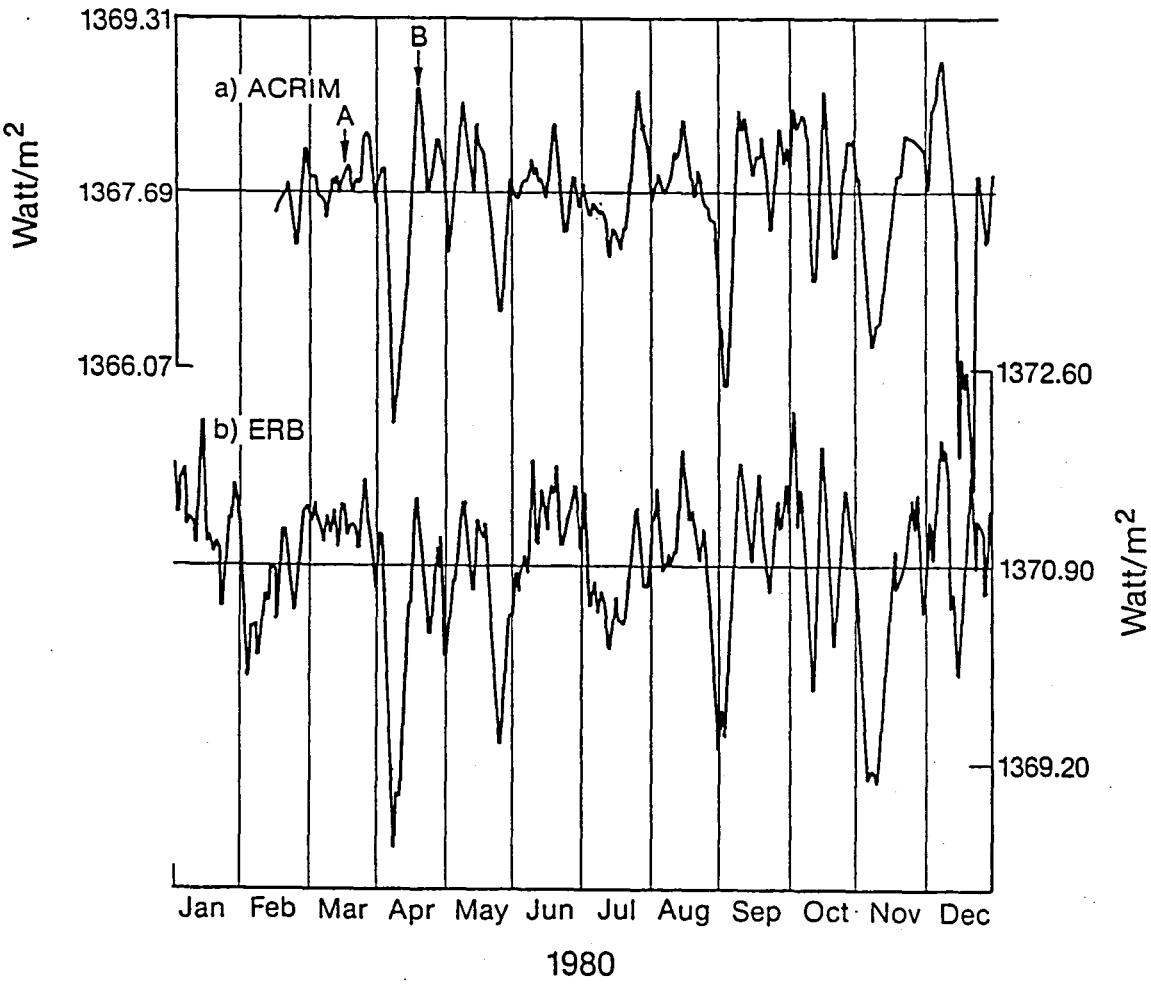
1369.31
B
a) ACRIM
A
1367.69
1366.07
Watt/m2
b) ERB
1372.60
1370.90
1369.20
Watt/m2
Jan Feb Mar Apr May Jun Jul Aug Sep Oct Nov Dec
1980

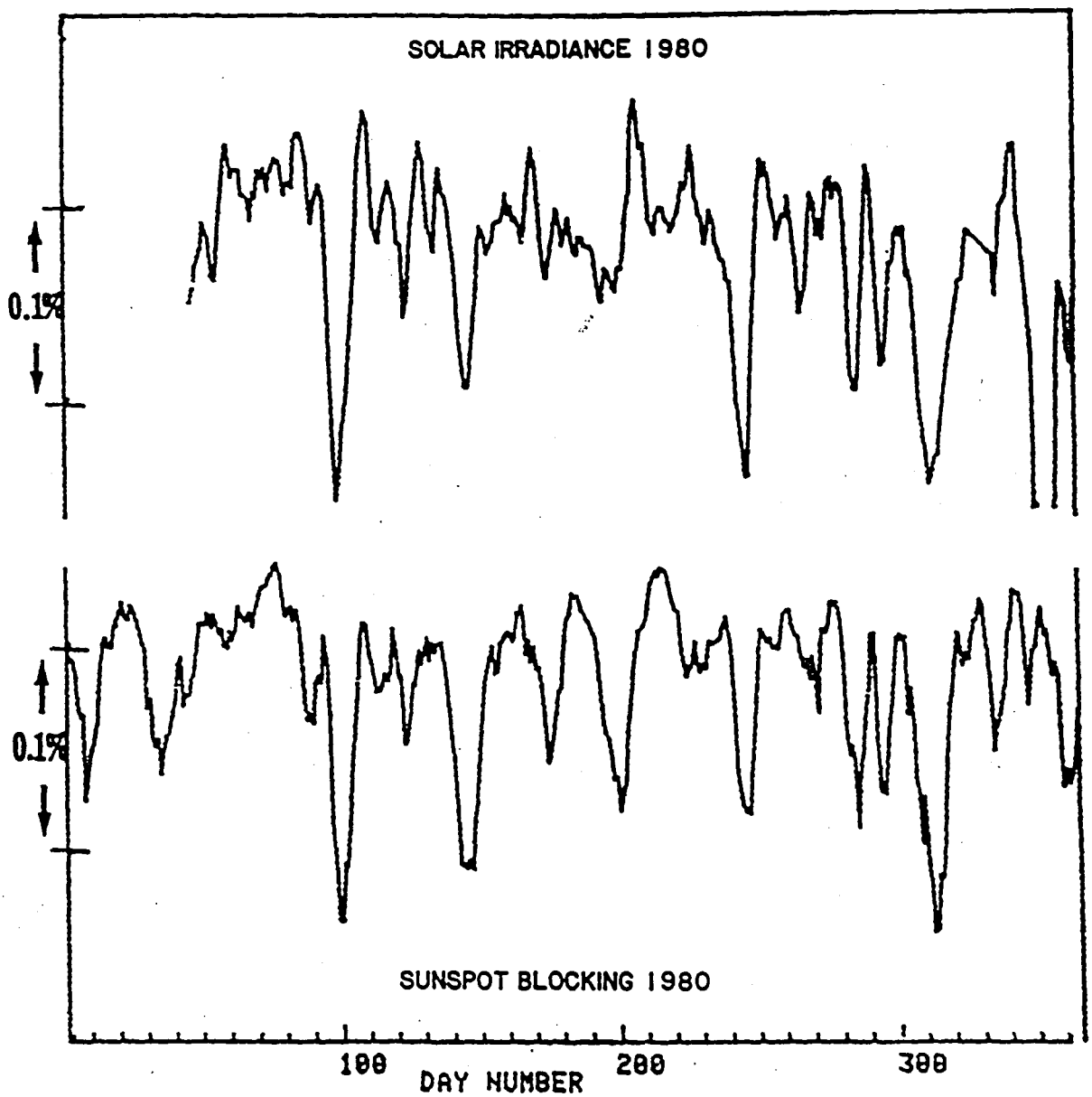
SOLAR IRRADIANCE 1980
0.1%
0.1%
SUNSPOT BLOCKING 1980
100
200
300
DAY NUMBER

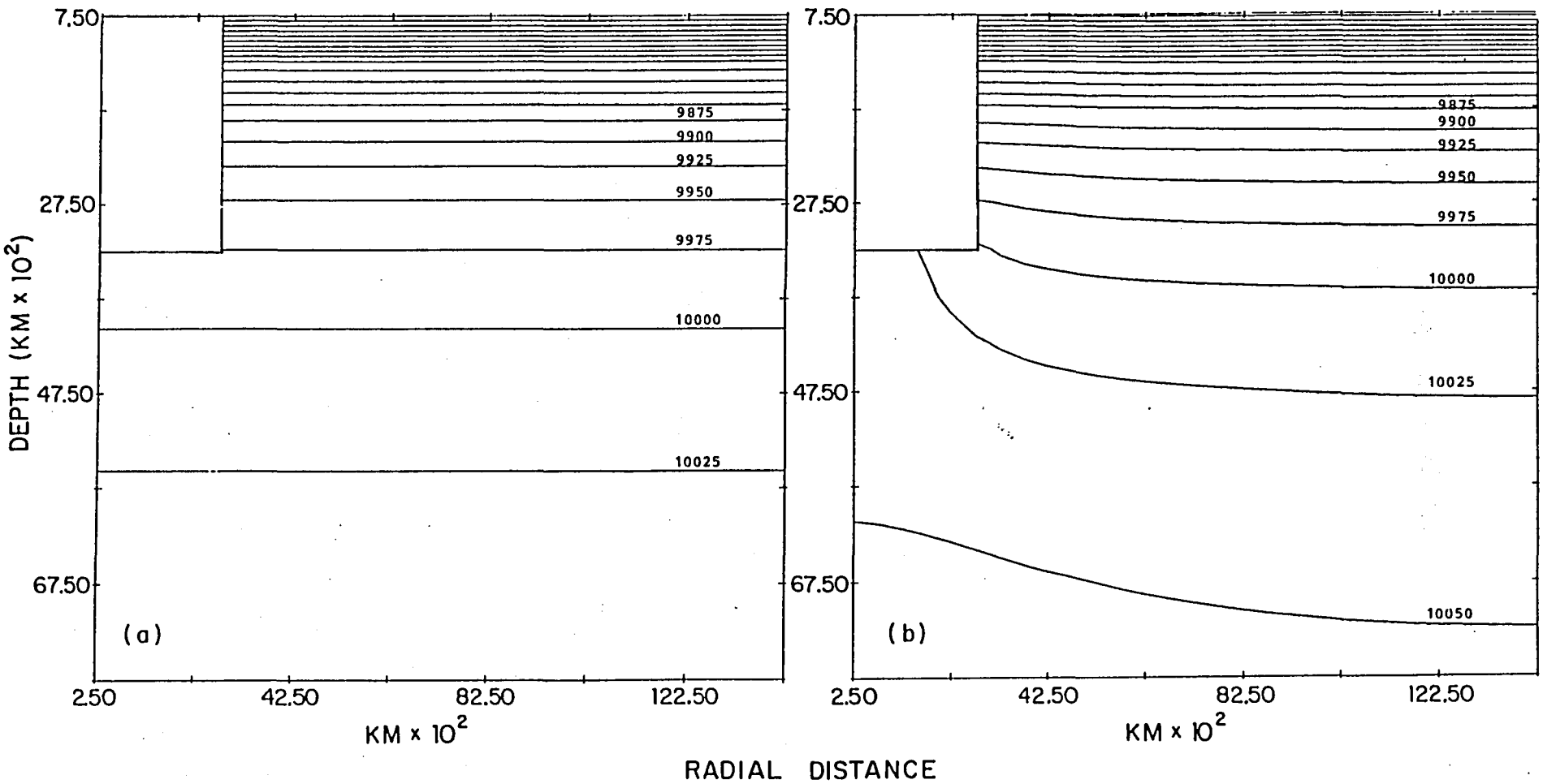
7.50
27.50
47.50
67.50
DEPTH (KM x 10²)
9875
9900
9925
9950
9975
10000
10025
(a)
2.50
42.50
82.50
122.50
KM x 10²
7.50
27.50
47.50
67.50
9875
9900
9925
9950
9975
10000
10025
10050
(b)
2.50
42.50
82.50
122.50
KM x 10²
RADIAL DISTANCE

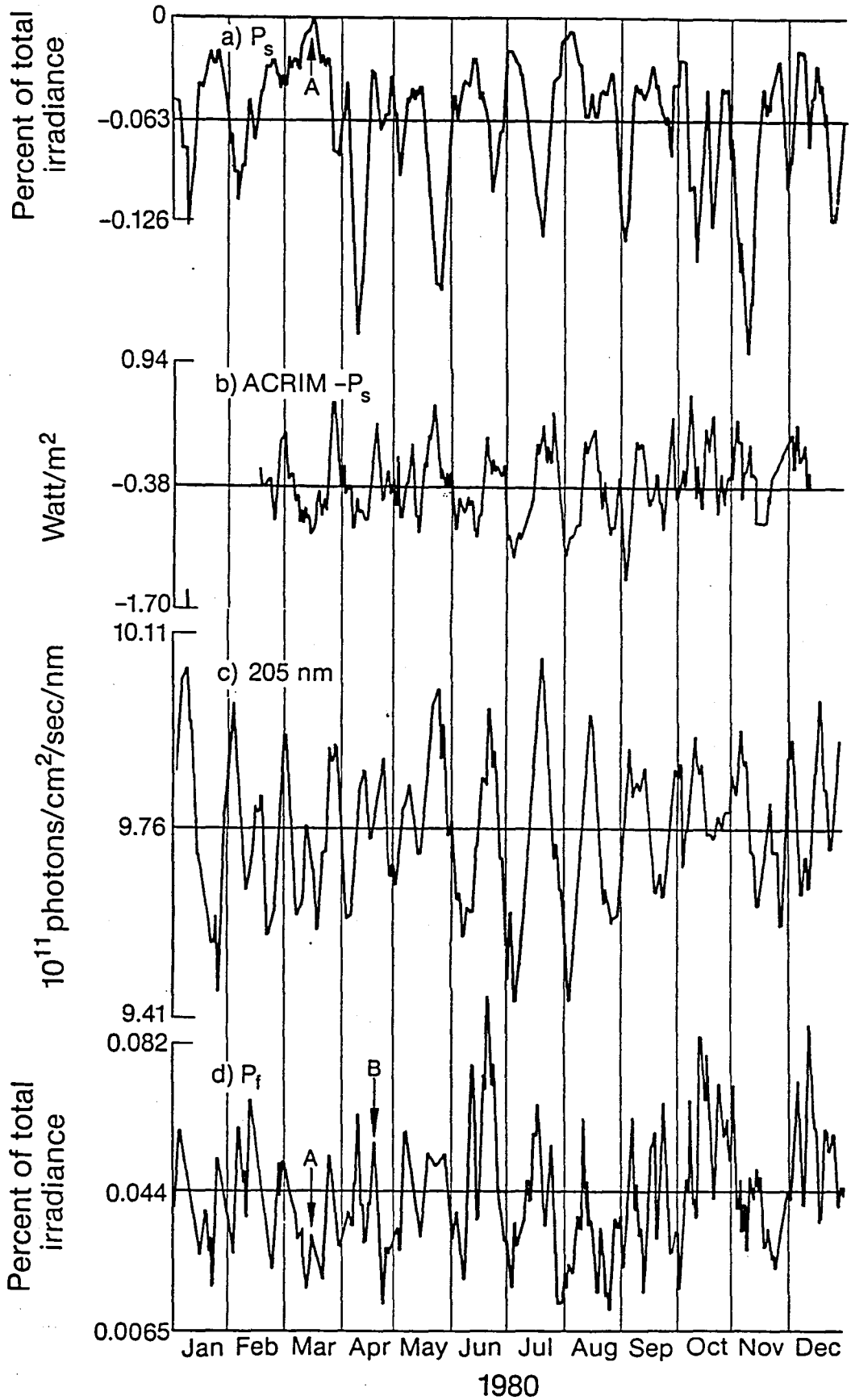
Percent of total irradiance
0
-0.063
-0.126
a) P_s
A
0.94
-0.38
-1.70
b) ACRIM -P_s
Watt/m^2
10.11
9.76
9.41
c) 205 nm
10^{11} photons/cm^2/sec/nm
0.082
0.044
0.0065
d) P_f
A
B
Percent of total irradiance
Jan Feb Mar Apr May Jun Jul Aug Sep Oct Nov Dec
1980

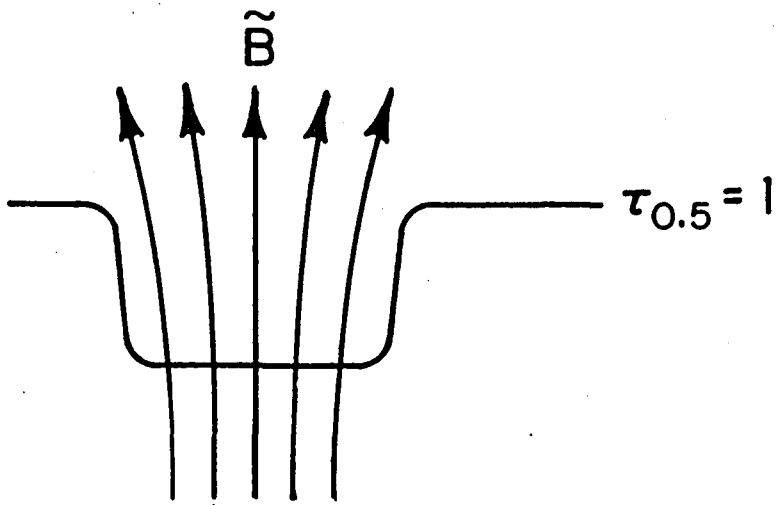

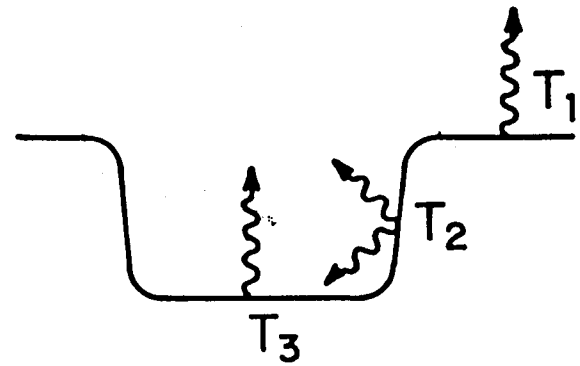

$T_2 > T_1$

$T_3 \gtrsim T_1$

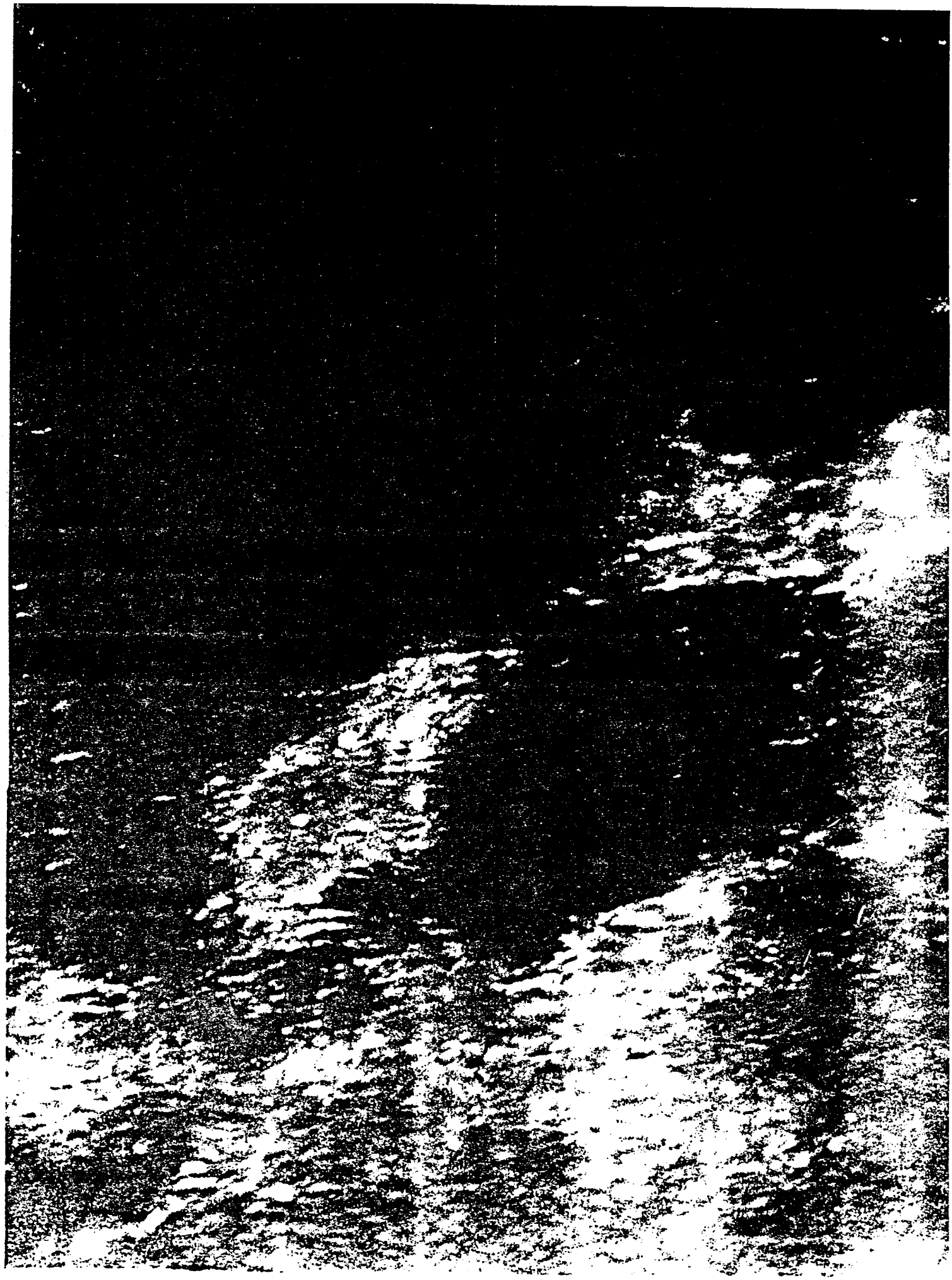

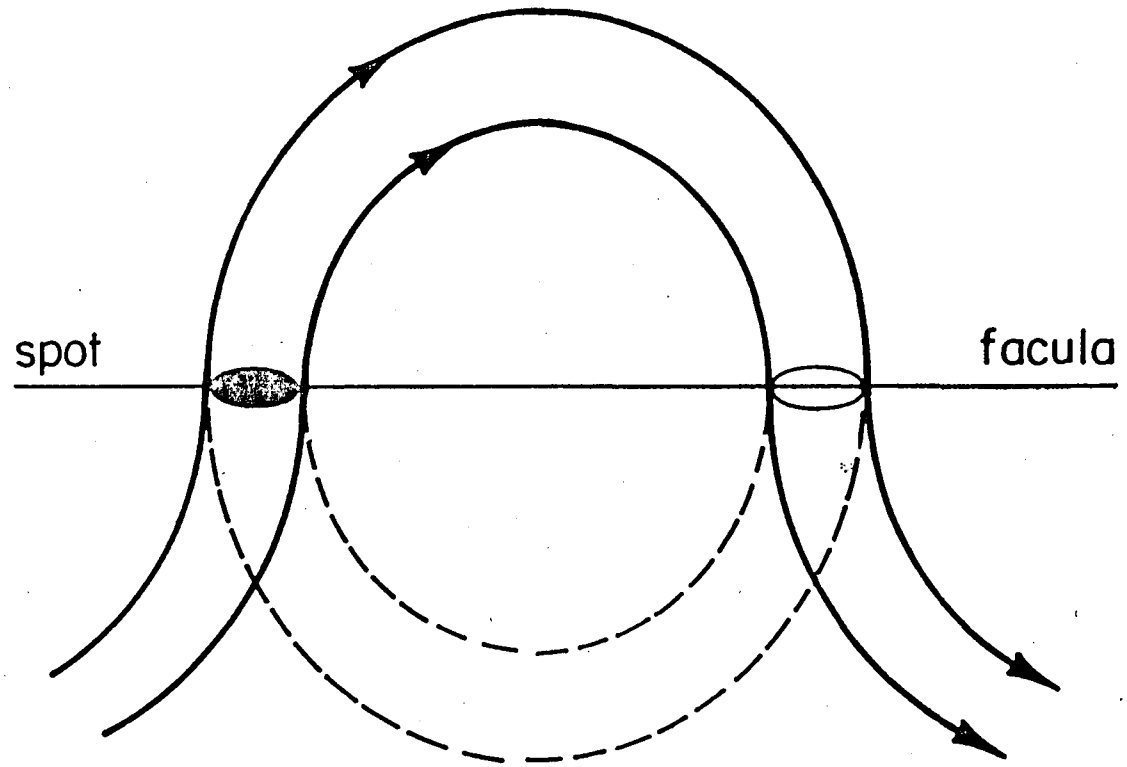
spot
facula

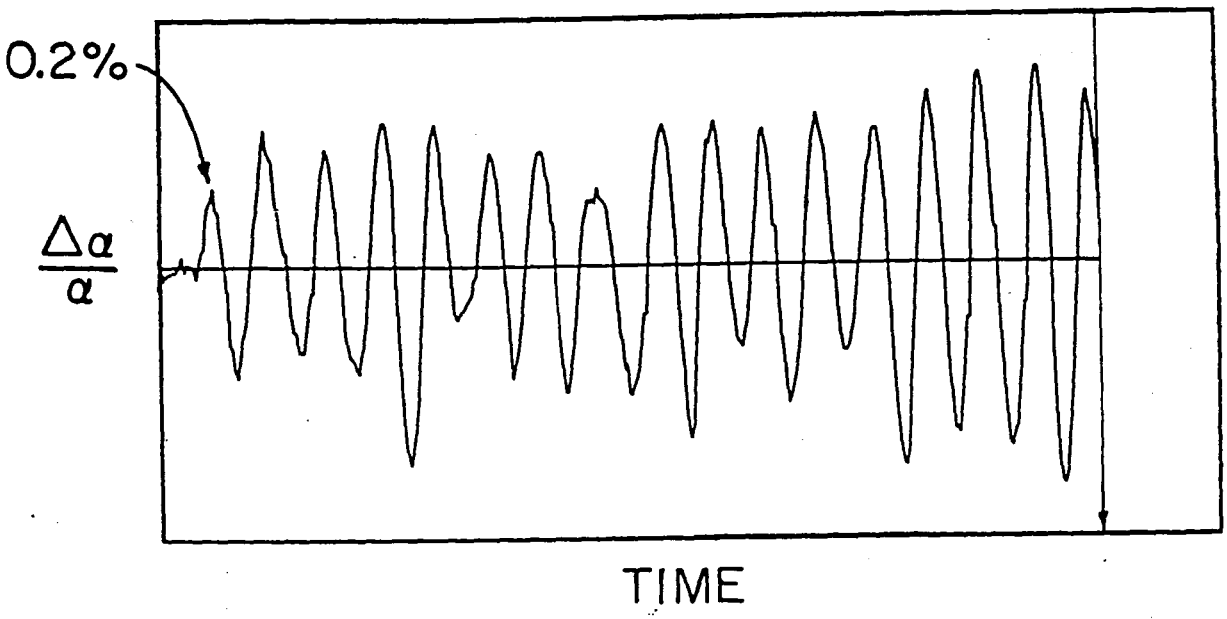
0.2%
$\frac{\Delta\alpha}{\alpha}$
TIME

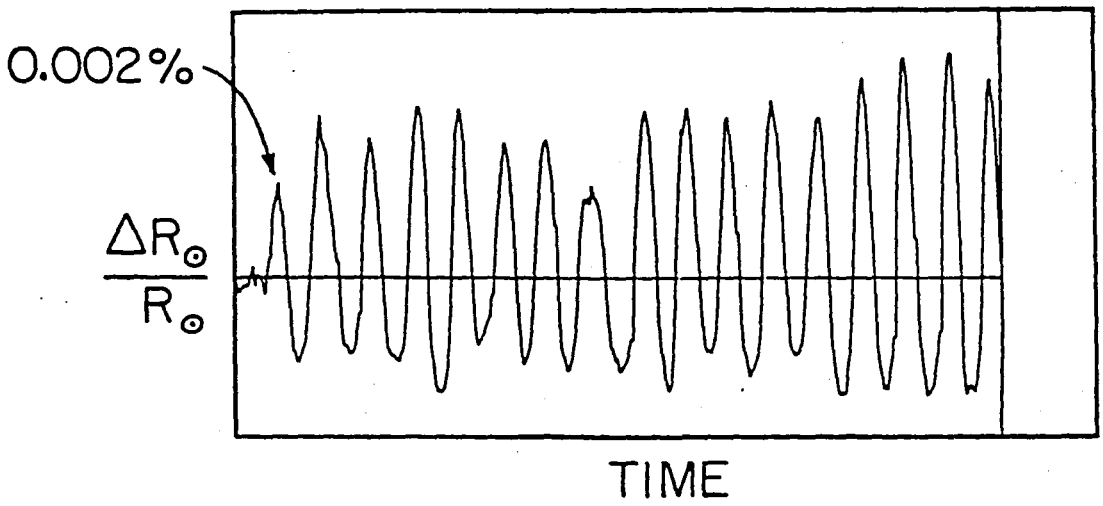
0.002%
$\frac{\Delta R_\odot}{R_\odot}$
TIME

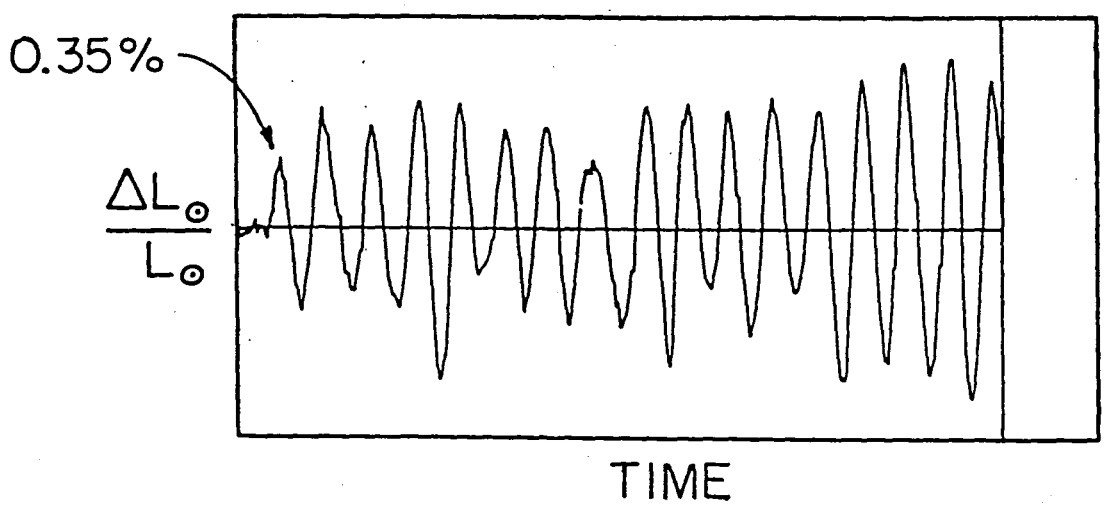
0.35%
$\frac{\Delta L_\odot}{L_\odot}$
TIME

End of Document